Characterization and Densification of Carbonized Lignocellulosic Biomass

Magnus Rudolfsson
Faculty of Forestry
Department of Forest Biomaterials and Technology
Umeå

Doctoral Thesis
Swedish University of Agricultural Sciences
Umeå 2016

Acta Universitatis Agriculturae Sueciae
2016:61

Cover: Pellets from torrefied pine wood
Photo: Magnus Rudolfsson

ISSN 1652-6880
ISBN (print version) 978-91-576-8624-4
ISBN (electronic version) 978-91-576-8625-1

Print: 2016

Characterization and Densification of Carbonized Lignocellulosic Biomass

Abstract

This thesis focuses on developing two main areas: characterization and densification of carbonized lignocellulosic biomass.

Thermally treated biomass undergoes changes that enrich the content of carbon in the remaining solid fraction. The carbon content is correlated to the temperature and residence time of the treatment and affects the properties of the material as a fuel e.g. gross calorific value. Near infrared (NIR) spectroscopy was used to predict a wide range of variables from forest- and agro-based biomass thermally treated at 240 to 850 ˚C. The result showed that NIR provided excellent predictions e.g. for energy, carbon, oxygen and hydrogen contents.

The changes of the biomass properties after thermal treatment, such as torrefaction, change also the pelletizing properties. A parametric study was conducted at bench scale in a single pellet press tool where four parameters were examined with respect to pellet quality responses. The study showed a narrow process window for pelletizing at around 5% moisture content. Further pelletizing studies in pilot scale demonstrated that higher moisture contents were needed for satisfying pellet quality. This indicated that there is a discrepancy between the material's moisture content before pelletizing and at the actual moment of feed layer formation and pelletizing. By drying both torrefied and untreated material it was shown that torrefied materials dried at a significantly higher rate. Thus, observed uneven pellet production caused by feed layer breakage was related to the drying rate due to heat from friction in the pellet press channels. This was demonstrated by developing two methods for cooling the pelletizing process: one with direct cooling by water injection and one with indirect cooling by coils in the die, and hereby reduce drying and keep the moisture content at a level where pelletizing was possible. This showed that cooling of the pelletizing process can be beneficial for the pellet quality.

The overall result for successful densification of thermally treated lignocellulosic biomass into a standardized commodity with high energy and bulk density stresses the need: (1) to find tools that characterize biomass facilitating suitable settings in the densification step; (2) to apply new innovative steps in sub-processes like cooling of the feed layer; and, finally, (3) to find matching combinations of torrefaction and pelletization.

Keywords: Norway spruce, Scots pine, willow, forest residues, reed canary grass, NIR, IR, thermal treatment, torrefaction, densification, pelletization, bench scale, pilot scale

Author's address: Magnus Rudolfsson, Swedish University of Agricultural Sciences, Department of Forest Biomaterials and Technology, SE-901 83 Umeå, Sweden, E-mail: magnus.rudolfsson@slu.se

Till Stina, Greta, Kerstin och Erik

It's a Long Way to the Top (If You Wanna Rock 'n' Roll)
AC/DC

Contents

List of Publications

This thesis is based on the work contained in the following papers, referred to by Roman numerals in the text:

I. Lestander, T.A., Rudolfsson, M., Pommer, L., Nordin, A. (2014). NIR provides excellent predictions of properties of biocoal from torrefaction and pyrolysis of biomass. *Green Chemistry*, 16(12), pp. 4906-4913.

II. Rudolfsson M, Stelte W., Lestander T.A. (2015). Process optimization of combined biomass torrefaction and pelletization for fuel pellet production – A parametric study. *Applied Energy* 140 378–384

III. Larsson, S.H., Rudolfsson, M., Nordwaeger, M., Olofsson, I. & Samuelsson, R. (2013). Effects of moisture content, torrefaction temperature, and die temperature in pilot scale pelletizing of torrefied Norway spruce. *Applied Energy*, 102, pp. 827-832.

IV. Rudolfsson M., Borén E., Pommer L., Nordin A., Lestander T.A. (2016). Effects of combined parameters for torrefaction and pelletization on wood pellet quality. Submitted manuscript.

V. Larsson, S.H., Rudolfsson, M. Temperature control in energy grass pellet production - Effects on process stability and pellet quality. *Applied Energy* 97 (2012) 24-29.

VI. Rudolfsson M., Larsson S.H., Lestander T.A. (2016). New tool for improved control of sub-process interactions in rotating ring die pelletizing of torrefied biomass. Manuscript.

Magnus Rudolfsson's contributions to the papers included in this thesis were as follows:

I The authors planned the experimental work together. Rudolfsson collected materials and conducted the NIR spectroscopy, carried out most of the analysis, evaluated the results and wrote parts of the paper.

II Rudolfsson carried out all analysis (except the compression and friction data collection, which was done at DTI in Denmark), evaluated the results and wrote the paper.

III Rudolfsson planned and carried out most of the pelletization work, contributed to the analysis, and helped to write the paper.

IV Rudolfsson and Borén contributed equally to the planning and the preparation of torrefied materials, as well as to the experimental work on pelletization. Rudolfsson contributed to evaluation of all MLR results and to the writing of large parts of the paper.

V Rudolfsson planned and conducted the experimental work, evaluated large parts of the results, and contributed to writing the paper.

VI Rudolfsson planned and conducted the experimental work and together with the other authors evaluated the results and wrote the paper.

Paper III was included in the PhD thesis of Martin Strandberg (2015): From torrefaction to gasification. Doctoral Thesis, Umeå University, Department of Applied Physics and Electronics, Umeå, Sweden. ISBN: 978-91-7601-287-1.

Abbreviations

c_v	Coefficient of variation
DoE	Design of experiments
EMC	Equilibrium moisture content
F_{max}	The maximal force needed to overcome static friction
FT-IR	Fourier transform infrared
GCV	Gross calorific value
MLR	Multiple linear regression
NIR	Near infrared
PCA	Principal component analysis
PLS	Partial least squares
Py-GC/MS	Pyrolysis–gas chromatography/mass spectrometry
RCG	Reed canary grass
SPC	Sweden Power Chippers
TGA	Thermogravimetric analysis
W_{comp}	Work required to compress biomass into a pellet (750 mg)
W_{fric}	The energy required to push the pellet through the press channel (kinetic friction work)

1 Introduction

Over the last 11,700 years, the planetary boundaries that have enabled the maintenance of a Holocene-like state of the earth system have supported the development of human societies. Steffen et al. (2015) and others have identified climate change, due to anthropogenic emissions of greenhouse gases like carbon dioxide (CO_2), as one boundary that has the potential on its own to drive the Earth system into a new state. This change may be persistent and lead to future states that are much less hospitable to the development of human societies (Schneider, 2004; Solomon *et al.*, 2009; IPCC, 2013). The current trajectory threatens to overrule safe planetary boundaries: in every year over the last half-century, the Mauna Loa observatory in Hawaii has reported new record levels of accumulated atmospheric CO_2 (NOAA, 2015); the cumulative anthropogenic emissions of CO_2 since the beginning of industrialization are approaching four trillion tonnes (Allen *et al.*, 2009), or about 598 Pg C (according to trillionthtonne.org, accessed 2016 February); the proportion of atmospheric CO_2 originating from fossil fuel combustion and cement production has grown by 2.5% over the last decade (Friedlingstein *et al.*, 2014); recent global observations of top-of-atmosphere fluxes show that the Earth's energy is imbalanced by 0.6 W m^{-2} on average; and the global consumption of fossil energy is expected to increase in line with the expected 30% increase in population growth by 2050 (UN, 2013).

To ensure that the expected global warming caused by greenhouse gas emissions will not raise the average global temperature by more than 2 °C above the pre-industrial average, McGlade & Ekins (2014) state that no more than one third of all current global fossil fuel reserves may be used up to the year 2050. This operating space corresponds to around 300 Pg of carbon released as 1,100 Pg CO_2 (Meinshausen *et al.*, 2009), or less than 10 Pg C per year. If more fossil carbon is used in energy conversion and emitted into the atmosphere as CO_2, this limit of 2 °C will be exceeded.

The Paris agreement of 2015 (UNFCCC, 2015) clearly marked the end of the beginning of the new Anthropocene epoch (Ruddiman *et al.*, 2015). For the first time, the world's leaders indirectly agreed that mankind has the power to control the global climate when they decided to restrict the increase in the global average temperature to less than 2 °C above pre-industrial levels. This will reduce the risk of exceeding critical planetary boundaries and help to mitigate the impact of climate change.

The world's terrestrial gross primary production (mainly due to plant growth) is about 109-150 Pg C y^{-1} (Still *et al.*, 2003; Zhao *et al.*, 2005; Sasai *et al.*, 2007; Beer *et al.*, 2010; Yuan *et al.*, 2010; Jung *et al.*, 2011; Ryu *et al.*, 2011); the most recent estimate is 128.2 ± 1.5 Pg C y^{-1} for the period from 2000 to 2010 (Yan *et al.*, 2015). Tao *et al.* (2012b) estimated that the globally available potential for energy conversion of agro-based residual biomass was 6.7 Pg, which corresponds to about 5% of the annual terrestrial gross primary production. Thus, this renewable resource of biomass from plants is considered to be CO_2 neutral and can compensate for gaps in the energy supply created by limitations on the use of fossil resources (Ragauskas *et al.*, 2006). A more complex picture of the biomass as CO_2 neutral is presented by Johnson (2009) where biomass of different sources do not have the same carbon footprint especially when it comes to combustion. Lignocellulosic biomass being renewable only accounts for approx. 10% of the global energy supply compared to 78% for fossil fuels (REN21, 2015). In Sweden bioenergy is now the dominating energy source with 33.6% of the total domestic energy use in 2013 (Svebio, 2016).

All this calls for urgent large scale development and implementation of sustainable biobased systems. It is necessary for large scale biomass supply systems to be based on homogenization and densification (Stephen *et al.*, 2010; Tumuluru *et al.*, 2011) because biomass is heterogeneous, with low and variable energy densities. Large-scale global transport systems of this sort have already been developed for animal feed. An important goal is to create biomass fuel units with a high mass and energy density, physical uniformity, and good flowability in handling systems. Pellets have these features and over the last few decades, technical systems have been adapted to accommodate the use of pelletized lignocellulosic biomass as a feedstock for energy conversion to produce heat (and also power in biocombines), and for biorefinery production of biofuels, green chemicals and other biobased products.

Fuel pellets from lignocellulosic biomass are one of the fastest growing energy commodities in the world. The global production of pellets from wood in 2014 was 27 Tg (million tonnes) (Kummamuru, 2015) and the yearly global

demand for wood pellets is expected to increase to over 100 Tg by the year 2020 (Sikkema *et al.*, 2011). The ISO standard 17225-2:2014 classifies wood pellets for energy combustion according to their dimensions, mechanical durability, bulk density, and contents of fines, ash, and additives. Moreover, an ENplus quality certification scheme has been introduced to establish stricter quality criteria for wood pellets (EPC, 2015).

A pretreatment process that may facilitate the transformation of lignocellulosic biomass into a globally relevant energy commodity is torrefaction, or mild pyrolysis at temperatures of 200 to 350 °C under low partial pressures of oxygen. Pyrolysis can improve the quality of lignocellulosic feedstocks by reducing their inhomogeneity, bio-contamination, and resistance to grinding (Repellin *et al.*, 2010) as well as their oxygen content, which will increase the energy density per unit mass of the remaining biomass. All of these factors are important for further thermal, thermochemical and biochemical processing (Meng *et al.*, 2012; Sheikh *et al.*, 2013). Torrefaction also reduces the hydrophilicity of the biomass (Bourgois & Guyonnet, 1988; Bergman *et al.*, 2005) by inducing the decomposition of sites where water molecules could form hydrogen bonds with the material. Thermally treated materials therefore have lower equilibrium moisture contents than their untreated counterparts. Kymäläinen *et al.* (2015) have shown that undensified torrefied material has voids that can be filled with free water, for example when the material is exposed to rain, leading to capillary moisture absorption. Pelletizing torrefied materials to a density close to that of the tissue (the material's so-called true density) will reduce the number and size of these voids, producing a carbonized commodity with improved and uniform quality. This will also reduce the costs of handling, transport and subsequent conversion. The development of standardized energy and biochemical carriers as globally tradable commodities that can serve as a renewable equivalent of crude fossil fuel will thus be a key step in the transition to a biobased economy.

However, the production of pellets from torrefied wood is currently a process in pre-commercial development. Classifications for thermally treated biomass have recently been incorporated into an international standard (EN ISO 17225-1:2014), with some alterations relating to parameters such as moisture content, and bulk density, and some additional factors such as fixed carbon content and volatile matter. In addition, there is ongoing work on finalizing standards for thermally treated densified biomass within the standard (prEN ISO 17225-8), particularly on methods relating to hydrophobicity, grindability, and moisture uptake that have been suggested for inclusion (Alakangas, 2014; Witt *et al.*, 2015).

Many challenges remain to be overcome before all the benefits of torrefied biomass in pelletizing can be fully utilized. Peng *et al.* (2015) concluded that instead of torrefying pellets, it is better to focus on pelletizing torrefied biomass and try to develop processes that have low energy consumption but still yield durable pellets by optimizing the die channel design, roll pressure and pelletizing process temperature. The major challenges are: (i) the amount of energy required to pelletize torrefied biomass is often greater than that needed to produce conventional wood pellets (Stelte *et al.*, 2011; Li *et al.*, 2012); (ii) particles of torrefied biomass are not as easy to bind effectively as those from untreated biomass (Peng *et al.*, 2013); (iii) significant amounts of fines and dust are often produced during pelletization (Larsson *et al.*, 2013); (iv) decreased pellet durability (Jarvinen & Agar, 2014); and (v) the production window may be narrow, which adversely affects predictability and the consistency of product quality (Koppejan *et al.*, 2012).

The overall aim of the work presented in this thesis was thus to generate knowledge that will support the development of techniques for rapidly characterizing carbonized biomass in order to monitor variation in the material, and to evaluate process parameters relevant to the densification of carbonized biomass, with particular emphasis on the pelletization of torrefied biomass. The specific objectives of the thesis are presented in Section 1.6.

1.1 Composition of lignocellulosic biomass

The main structural components of lignocellulosic biomass are cellulose, hemicelluloses and lignin. In addition, there are smaller amounts of non-structural components such as extractives and inorganic ash-forming elements. This biomass originates from a wide range of different sources such as woody materials, herbaceous grasses and plants, aquatic plants, and various waste streams from industrial processes. The source of the biomass has a large impact on its chemical and structural composition. For example, Vassilev *et al.* (2012) reported large variations in the composition of wood, whose contents of cellulose, hemicellulose, and lignin ranged from 12.4 to 65.5 % (mean 39.5%), 6.7 to 65.6 % (mean 34.5%), and 10.2 to 44.5% (mean 26.0%), respectively. This variation is due to differences in species, tissue type, growth location, soil conditions, and so on.

In the composite structure of lignocellulosic biomass, cellulose forms fibrils that act as stiff reinforced fibers in the plant cell walls, while hemicellulose and lignin constitute the soft matrix (*Figure 1*).

The wide variation in the contents of cellulose, hemicellulose and lignin in different biomass samples can give rise to different exothermal behaviours

during thermal processes such as torrefaction, potentially leading to temperature runaways (Di Blasi *et al.*, 2014). Together with difficulties in process control, this variation can produce uneven process outcomes.

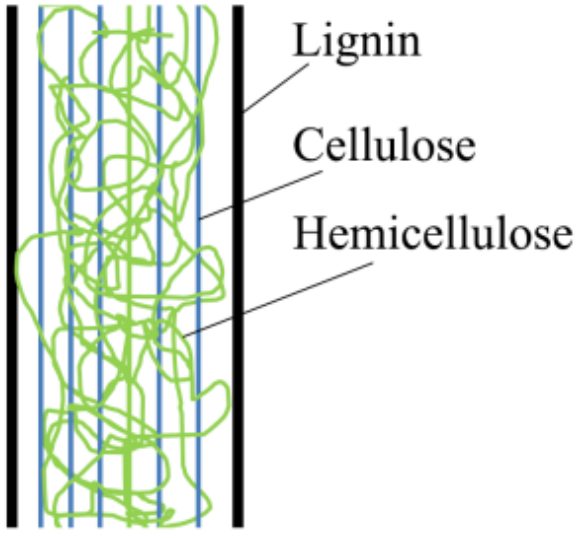

Figure 1. Schematic picture of lignocellulosic biomass cell wall composition. Adapted from Mosier *et al.* (2005)

1.1.1 Cellulose

The most abundant natural polymer in the world is cellulose – a polymer that consists of glucose ($C_6H_{10}O_5$) molecules linked in linear chains of 300 to 1,700 units and is found in materials such as wood pulp (Klemm *et al.*, 2005). Chains with significantly more monomer units (between 7000 and 15 000) have also been reported (Gibson, 2012)

The individual glucose molecules within each cellulose chain are covalently bonded to one-another, and the chains are interconnected by hydrogen bonds, resulting in the formation of multi-layered flat ribbon-like structures connected by hydrogen bonds. These basic bundles of cellulose molecules form microfibrils; the number of cellulose chains per microfibril was calculated by Fink *et al.* (2001) to be as high as 1000 in larger aggregates of pulp microfibrils. Similarly, Sugiyama *et al.* (1985) found that cellulose microfibrils produced by a marine alga contained 1200-1400 cellulose chains. However, according to Hatfield (1993), the cellulose microfibrils of forage plants contain only around 70 cellulose chains. These microfibrils form the fundamental skeletal component of the plant cell wall and have high axial stiffness. They also have regions with disordered chains (amorphous regions) and others with

highly ordered chains (crystalline regions), which increases their ability to withstand bending forces. Bundles of microfibrils form fibrils, which are the main constituents of cellulose fibres. Networks of such fibrils in the cell wall matrix are the key components of the plant's structural reinforcement.

The relatively high oxygen content of cellulose means its energy content is lower than that of lignin and extractives. Gross calorific values of 17.03 and 17.43 kJ g^{-1} (Murphey & Masters, 1978) have been reported for cellulose from extracted oak wood, while the gross calorific value of pure Avicel ($C_6H_{10}0_5$) is 17.34 ± 0.11 kJ g^{-1} (Domalski & Milne, 1987).

1.1.2 Hemicellulose

Unlike the linear structure of cellulose, hemicellulose is branched and contains many different sugar monomers, including the pentoses xylose and arabinose and the hexoses glucose, galactose, mannose and rhamnose. The structures of individual hemicellulose molecules are quite variable; some are heavily branched while others have only short side chains. Xylan is the most common hemicellulose in the cell walls of hardwoods in particular, and contains mostly xylose. In softwoods, glucomannan is the most common hemicellulose. A wide range of hemicelluloses have been identified, with different types being found in different species, tissues and locations in the cell wall. Individual hemicellulose molecules typically have 80-200 hexose and pentose monomers, and their branching tends to favour loose packing. Native hemicellulose is therefore amorphous and more reactive than cellulose. The solubility of hemicelluloses increases with their degree of branching, and with their content of hydroxyl (O-H) groups available for hydrogen bonding with solvents like water.

Chemical pulps contain residual fragments of short-chain hemicelluloses even after extended cooking, suggesting that the molecular backbones of at least some hemicelluloses are attached to cellulose microfibrils. Walker (2006) reports that both ends of the branched chains of glucomannans and xylans can bind to microfibrils, leading to the formation of snakelike patterns of relatively inflexible chains. These bridges between hemicelluloses and cellulose microfibrils may help to separate the fibrils and prevent them from sliding apart, thereby increasing the stability of the network in the cell wall. Because lignin also binds to hemicelluloses in the cell wall, hemicellulose represents a link between cellulose and lignin. It has therefore been suggested that hemicellulose redistributes stresses when the cell wall is subjected to dynamic and static forces (Walker, 2006).

The energy content of hemicelluloses is about the same as that of cellulose; Domalski & Milne (1987) reported that extracted hemicellulose from oak has a

gross calorific value of 16.67 kJ g^{-1}, whereas xylan ($C_5H_8O_4$) has a higher value of 17.75 kJ g^{-1}.

1.1.3 Lignin

Lignin is the second most abundant natural polymer in the world and is found in all higher plants. The spaces between cellulose, hemicellulose, and pectin molecules are filled with lignin, especially in the xylem cell walls. One of its functions is to increase the mechanical strength of the cell walls, which it achieves by forming covalent bonds with hemicellulose and thus enhancing the cross-linking of the cell wall's carbon matrix. In addition, because it is more hydrophobic than other structural components such as cellulose and hemicellulose, lignin is important for the conductance of water within the plant's tissues. The building blocks of native lignin are the three mono-lignols, p-hydroxyphenol (H), guaiacol (G) and syringol (S). These undergo condensation reactions to form amorphous complex cross-linked macromolecules with an undefined structure resulting from the formation of more or less randomized linkages in a 3-dimensional network.

Although exceptions exist, the lignins in hardwoods consist mainly of guaiacyl and syringyl building blocks with traces of p-hydroxyphenyl monomers, whereas softwood lignins consist mostly of guaiacyl units with low levels of syringyl and p-hydroxyphenyl components (Boerjan *et al.*, 2003). Normark (2014) found that the syringyl-guaiacyl ratio of different fractions of Scots pine ranged from 0.021-0.025, whereas Bose *et al.* (2009) found that the corresponding ratio in poplars ranged from 1.01 to 1. The levels of syringyl and guaiacyl units in lignins from grasses are quite similar, and these lignins have higher concentrations of p-hydroxyphenyl units than those in woody plants (dicotyledons) (Boerjan *et al.*, 2003).

The gross calorific value of lignin is higher than that of cellulose and hemicellulose. For example, lignins extracted from hardwoods and softwoods having empirical formulas of $C_{10}H_{l2}O_{4.2}$ and $C_{10}H_{l1.2}O_{3.3}$ were found to have gross calorific values of 24.69 and 26.36 kJ g^{-1}, respectively (Domalski & Milne, 1987). However, Murphy & Masters (1978) reported a value of only 21.18 kJ g^{-1} for extracted lignin from oak.

1.1.4 Non-structural components

Extractives and ash-forming elements in lignocellulosic biomass are non-structural components, in contrast to cellulose, hemicellulose, lignin and other organic components such as sugars, starch, pectin and protein. The extractives include a wide range of compounds that can be extracted using polar (e.g.

water) or non-polar (e.g. ether) solvents. The extractives of primary interest in this work are waxes, oils, fats, lipids, resins, tannins and other phenolics that are extracted by non-polar solvents. These components are volatile and devolatilize in thermal processes like torrefaction. They have high energy values with up to about 38 kJ g^{-1} for oils and fats. Their relative abundance varies between species and tissue types: knotwood in pine stems has a resin acid content of up to 45% (Boutelje, 1966), while the fruits of the oil palm contain around 30% oil.

High ash contents in lignocellulosic biomass increase the severity of operational problems such as fouling and slagging during thermal conversion, and elements such as sodium and potassium are especially unwanted in many thermal processes because they cause low ash melting temperatures (Miles *et al.*, 1996; Zevenhoven-Onderwater *et al.*, 2000; Boström *et al.*, 2012; Wang *et al.*, 2014). Biochemical processes are also influenced by ash elements; for example, elevated acid neutralization can reduce the conversion yields of xylose from maize stalks (Weiss *et al.*, 2010).

The ash content of biomass varies widely, from 0.2% in pure wood to 25% in rice straw according to a comprehensive review by Tao et al. (2012a). For maize (stalks, cobs and husks) and wheat (straw), Kenny *et al.* (2013) showed that the total ash content varied from 1 to 23%, with typical values of 7-9%. According to Obernberger *et al.* (2006), the typical ash contents of individual tree components range from 0.3% in wood to 5.0% in the bark, with the bark of pine, spruce and birch trees having ash contents of about 2-3% (Lestander *et al.*, 2012b). In addition, logging residues have ash contents of 1.5-2%, while the ash content of willow harvested after short rotation coppicing is around 2%. The most abundant ash element in plant biomass is Ca, followed by K, Si, Mg, Al, S, Fe, P, Cl, Na, Mn and Ti in decreasing order (Vassilev *et al.*, 2010).

1.2 Thermal treatment

The main drawback of biomass as an energy carrier relative to fossil fuels is its high oxygen content, which gives it a low calorific value. Its high moisture content and hydrophilic behaviour are also problematic during storage because a range of microbes will attack and degrade all wet biomass. To limit this growth of microbes, Jirjis (1995) concluded that the moisture content of biomass should be below 15%. The fibrous structure and heterogeneous nature of biomass are also major problems in many processes. Thermal treatment of biomass by torrefaction is a way to upgrade biomass into an improved energy carrier that is more suitable than raw biomass for use in downstream processes,

especially thermal processes like gasification and co-firing with coal (Prins *et al.*, 2006).

1.2.1 Torrefaction

Torrefaction is a controlled thermal treatment where the degree of decomposition of biomass depends on the reactor temperature and residence time. The first equipment for continuous torrefaction was manufactured for roasting coffee (Thiel, 1897; Offrion, 1900). The torrefaction of lignocellulosic biomass is performed at ambient atmospheric pressure and low partial pressures of oxygen, with reactor temperatures between 200 °C and 350 °C, and biomass residence times ranging from a couple of minutes up to hours depending on technique and desired degree of torrefaction (Yvan, 1985; Bourgois & Guyonnet, 1988; Bergman *et al.*, 2005; Nordin *et al.*, 2013; Grigiante & Antolini, 2015).

During torrefaction the biomass undergoes devolatilization, elemental dehydration and carbonization, making it into a more coal-like material and modifying the structures of its original components by reducing their atomic O/C and H/C ratios. The decreased O/C ratio increases the material's energy content. In addition, its ash content increases due to the loss of organic material.

Cellulose, hemicellulose and lignin decompose at different rates during torrefaction. The decomposition of hemicelluloses begins at temperatures of around 200 °C for xylan, for which the first degradation peak occurs at 243 °C. This peak is associated with the release of high levels of the off-gas CO_2 as a result of the decomposition process (Werner *et al.*, 2014). Unlike cellulose and most other hemicelluloses, xylan decomposes exothermally. The decomposition of other hemicelluloses (e.g. glucan and xyloglucan) produces a peak at 332 °C, at which point CO and other organic trace gases are formed; at higher temperatures, CH_4 is also given off. The degradation of cellulose begins at temperatures around 280 °C and is fastest at around 330 °C. (Werner *et al.*, 2014). Lignin consists of complex molecular networks whose decomposition begins at 230 °C and continues up to temperatures of about 900 °C (Melkior *et al.*, 2012). Lignin undergoes condensation, depolymerization, and demethoxylation reactions during torrefaction, and as the last component to degrade, its relative abundance increases as the torrefaction proceeds and the harshness of the conditions increases.

The degradation of the hemicellulose, cellulose and lignin matrix leads to a more brittle material. This will shift the product's size distribution towards smaller particles than those found in the untreated biomass, reducing the energy required to grind the material (Phanphanich & Mani, 2011; Strandberg

et al., 2015). These effects are beneficial for downstream processes such as densification by pelletization, entrained flow gasification and pulverized fuel burning where grinding is required.

1.3 Densification

Lignocellulosic biomass has a relatively low bulk and energy density together with high heterogeneity compared to conventional fossil fuels. For instance, the bulk density of sawdust is 200-350 kg m^{-3} and that of pellets is 550-700 kg m^{-3} (Strömberg & Herstad Svärd, 2012). A densification step is needed to make the feedstock into a more homogenous commodity with improved handling properties in various transport systems. Pre-treatment by torrefaction increases the energy content of the biomass but reduces its bulk density, creating a need for subsequent densification to reduce handling and transportation costs.

1.3.1 Pelletizing

Pellet plants producing wood pellets, a refined solid biofuel, receive raw material in the form of logs, chips and/or sawdust. This section briefly describes the pelletization process employed in most pellet plants that use untreated wood as their feedstock. More detailed reviews have been presented by Tumuluru *et al*. (2011) and Lestander (2013). Details of the individual steps in the process are provided in The Pellet Handbook (Obernberger & Thek, 2010).

If the incoming material consists of logs and/or chips, size reduction is required before any adjustment of its moisture content. However, if the unprocessed feedstock's particles are small, as in the case of sawdust, the conventional pelletizing process (see *Figure 2*) can be applied. The first step in this process typically involves drying the material to a moisture content of 6-14%. A grinding step is also usually needed to achieve a size distribution suitable for pelletizing. The raw material is then usually steam treated to soften the wood before pelletizing.

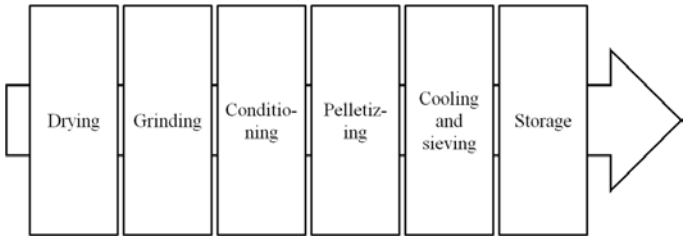

Figure 2. The conventional pelletizing process.

The most common pelletization method involves the use of a pellet mill with a rotating ring die and stationary free rolling rollers, see *Figure 3*. In this method, the material is fed into the die and continuously forced into the press nip between the die and the rollers, where a compressed feed layer is formed. The feed layer will also be attached to the inside of the rotating die, and as additional material is fed into the mill, the layers over the press channels will be successively extruded through each press channel. This will happen intermittently each time a roller passes over a channel. The consequence is that when new material enters the press channel, both static and kinetic wall friction must be overcome.

If the interfacial bonding within the feed layer and between the layer and the underlying die cannot withstand the roller's friction as well as compressing and shearing forces, the feed layer will disintegrate, causing an immediate production failure. This results in an uneven pellet mill motor load and production rate because when a new feed layer is built up, the die will be over-filled with material when the feed layer temporarily regenerates, causing the production rate to suddenly increase sharply. This phenomenon is described in detail by Larsson *et al*. (2012).

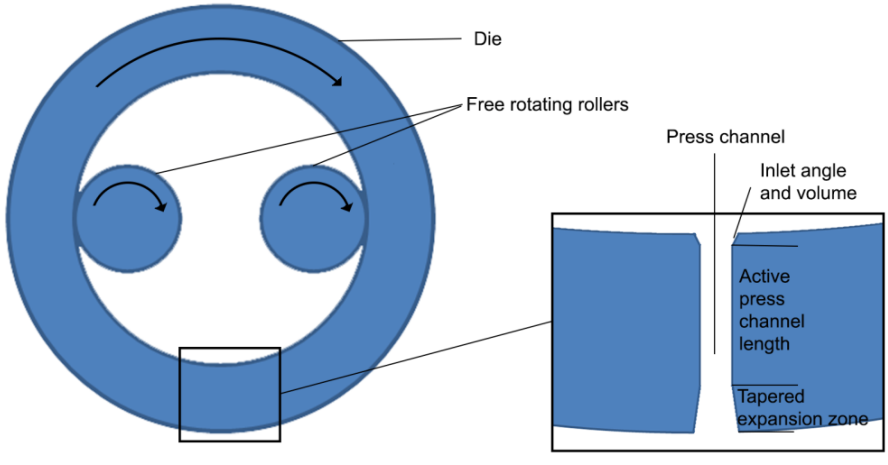

Figure 3. Schematic pictures of a ring die with rollers and a single die channel.

The pelletizing process is commonly divided into three phases, as shown in *Figure 4* (Pietsch, 2002; Tumuluru *et al.*, 2011). In phase one, the material is rearranged and closely packed together. In the second phase, the particles are forced against each other such that plastic and elastic deformations occur, followed by a third phase where further compression of the material results in a

density close to the material's true density. When the pellet exits the press channel, it will expand because of elastic spring back and/or compressed residual gas in the pellet. If the exit of the press channel is sharp, it may damage the pellet when it expands, so tapered exits are preferred (see *Figure 3*).

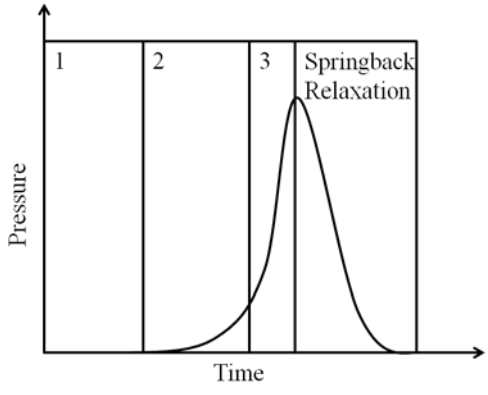

Figure 4. Pressure during the different phases of pellet compression.

The mechanical characteristics of pellets naturally depend on the composition of the pelletized material. In addition, the settings of the pellet press such as the press channel length and diameter will affect the friction between the material and the die, giving rise to different pelletizing pressures and temperatures (Kaliyan & Morey, 2009; Stelte *et al.*, 2011; Samuelsson *et al.*, 2012). Initial studies by Larsson *et al.* (2012) have shown that cooling the die is an effective way to overcome problems with discontinuous pellet production when pelletizing low bulk density straw materials in a ring die pelletizer.

The binding mechanisms between particles in pellets have been categorized into five main groups (Rumpf, 1962; Pietsch, 2002; Kaliyan & Morey, 2009; Samuelsson *et al.*, 2012):

(i) solid bridges
(ii) surface tension and capillary pressure (liquid bridges)
(iii) adhesion and cohesion forces (viscous binders, thin layers)
(iv) attraction forces between solids
(v) interlocking bonds (solids)

All of these forms of binding can develop simultaneously when biomass is pelletized, and many are favored by very small distances between particles and can be strong when fine material is densified. For instance, solid bridges form when lignin undergoes cooled recrystallization after being softened by

moisture and the heat that is developed during pelletization (Stelte *et al.*, 2012). Surface tension and capillary pressure are forces generated by the interactions between the particles and water. They can be strong, but disappear when the water evaporates at the high temperatures that occur during pelletization. Adhesion and cohesion forces exist if highly viscous binders and thin (<3 nm) adsorption layers are present. Examples of attraction forces between solids are van der Waals forces between transient dipoles on particles' surfaces, and hydrogen bridges between hydroxyl groups. Such forces also contribute to adhesion and cohesion. Another attractive force between solids is the valence force that may occur when fresh surfaces are created due to the breakage of particles during densification, which leaves unsatisfied valances at the newly formed surfaces. This can lead to the formation of strong bonds with other such surfaces. Interlocking happens when fibrous particles become entangled around one another during densification.

1.4 Charactarization of biomass

Biomass from lignocellulosic sources is far from homogeneous and there is a need for methods of on- or at-line characterization both before and after a process operation to monitor and adjust its parameters. Both inorganic and organic matters are of interest for process monitoring.

1.4.1 Infrared (IR) and near infrared (NIR) spectroscopy

Near infrared (NIR) spectroscopy is a non-invasive analytical method that uses near-infrared electromagnetic radiation in the 780-2500 nm range (Sheppard *et al.*, 1985). NIR radiation was first discovered in the year 1800 by Fredrick William Herschel (Davies, 1998). Infrared radiation interacts with polar chemical groups such as C-H, C-O, C=C and O-H in biomass, resulting in NIR overtones originating from the fundamental vibrations in the infrared (IR) spectral range, which extends from 4000 to 200 cm^{-1}. These overtone vibrations stem from atomic movements such as bond stretching and bending (Osborne, 1993). NIR absorbances are generally broader, more prone to overlapping, and less intense than IR absorbances, making the interpretation of NIR data challenging without the use of multivariate methods. Despite these drawbacks, NIR spectroscopy is widely used in the biomass industry (Lestander & Rhen, 2005; Lestander *et al.*, 2009).

Spectroscopic techniques for on-line characterization of feedstock properties can be used to monitor both ingoing materials (Axrup *et al.*, 2000; Li *et al.*, 2015) with respect to their chemical and structural components (e.g. cellulose, hemicellulose and lignin) and the outcome of the process.

1.4.2 Other spectroscopic techniques

Due to the unspecific nature of in particular NIR spectroscopy, finding additional sensors for relevant process variables are desirable. One possible candidate could be Raman spectroscopy as was shown by Ewanick *et al.* (2013) where they successfully used a novel immersion probe and a 785 nm laser in characterizing biobased materials.

Another candidate could be X-ray fluorescence (XRF) spectroscopy enabling characterization of ash related parts of the biomass on- or at-line (Thyrel *et al.*, 2013). Together with NIR the XRF technique can potentially be a more complete characterization configuration when installed in a biorefinery concept where both the ash content (inorganic parts) and composition together with the organic parts are of interest for downstream processes (Thyrel, 2014). Laser-induced breakdown spectroscopy (LIBS) is also a spectroscopic method that may be used for ash related analysis (Westover, 2013). Ash related problems are not within the scope of this thesis as the ash content rarely affects the pelletizing of biomass but it is of large interest when it comes to combustion due to e.g. ash melting and fouling.

1.4.3 Py-GC/MS

Py-GC/MS (pyrolysis–gas chromatography/mass spectrometry) is a chemical analytical method where the sample is heated to induce decomposition into smaller molecules that are separated by gas chromatography and then detected by mass spectrometry (Skoog, 1985). In the pyrolysis step, the organic compounds are decomposed into smaller components in the absence of oxygen. The subsequent gas chromatographic step involves using a column to separate the components of the analysed compound. The column is a narrow heated tube filled with a material that is referred to as the stationary phase. A gas stream, called the mobile phase, carries the constituents of the sample through the column.

Depending on the chemical and physical properties of the components and their interactions, with the stationary phase they will exit the column at different times; the time a given compound takes to pass through the column is known as its retention time. The temporal separation of individual compounds can be affected by the specific properties of the stationary phase and the temperature of the column. In a mass spectrometer, the sample is ionized by an ionization source, which may cause it to break up into smaller charged fragments. The ionized products are then accelerated in a magnetic field, causing species with different mass-to-charge ratios to be deflected to differing extents, giving rise to different signals for different compounds.

1.5 Multivariate statistics

NIR and other spectroscopic methods as well as chemical analyses like Py-GC/MS generate huge amounts of data and the numbers of observations are far smaller than the number of variables, where the observations correspond to the samples and the variables correspond to (for example) all of the datapoints in their spectra. Multivariate data analysis makes it possible to extract meaningful information from such data. Principal component analysis (PCA) can be used to obtain an overview of the data, determine which observations deviate from the others, and analyse the relationships among observations. The groupings identified in an initial PCA can be used to classify new samples and identify samples that do not fit into the established groupings, which may merit further investigation. Having performed such analyses, it may be useful to perform a regression analysis using a technique such as MLR.

1.5.1 Design of experiments (DoE)

Design of experiments (DoE) is a systematic method originally developed by Fisher (1935) for conducting experiments within a defined model space that is often defined around a particular central experiment. It is particularly useful in industrial contexts where it is imperative to minimize the number of individual experiments that are performed because of cost and time constraints. Various geometrical distributions of sample points within the model space can be used (e.g. cubic or onion distributions), depending on the goal of the study and the specific type of experiment to be conducted. The first step in the DoE process is to identify factors, i.e. variables that affect the system such as temperature, retention time and particle size in the case of torrefaction. The factors can be quantitative, qualitative, and uncontrolled. Responses are variables that are measured during and after the experiment; in a pelletization DoE design, responses of interest could include durability, bulk density and pellet temperature. Once the factors and responses have been identified, a number of experimental runs are selected representing different geometrical distributions of sample point positions within the chosen model space. DoE is useful in a wide range of applications including screening and optimization studies as well as model robustness testing (Eriksson *et al.*, 2008). Repetition of reference experiments, which are often referred to as centre points, is very important in DoE because their results are used to estimate the inherent variability and experimental error of the model. Another important feature is the randomization of the experiments. Multiple linear regression (MLR) and partial least squares (PLS) regression are commonly used to estimate the influence and significance of individual factors as well as factor-to-factor interactions.

1.5.2 Multiple linear regression (MLR)

Multiple linear regression (MLR) is an extension of classical linear regression with the exception that in MLR there are two or more predictor variables (often referred to as factors) that are used to model a dependent variable, which is typically referred to as a response. In MLR, ordinary least squares (OLS) are used to minimize the differences between observed and predicted values in the model. MLR modelling of a response **y** (e.g. pellet durability, density etc.) can be described by

$$\mathbf{y}=\mathbf{Xb}+\mathbf{f} \qquad \text{(Eq.1)}$$

where **y** is the vector of the measured mean-centred response, **X** is the mean-centred matrix of factors from the observations, **b** is the vector of regression coefficients obtained by OLS, and finally **f** is a vector of residuals.

The regression coefficients are estimated using Eq. 2.

$$\hat{\mathbf{b}} = (\mathbf{X}^T\mathbf{X})^{-1}\mathbf{X}^T\mathbf{y} \qquad \text{(Eq. 2)}$$

where $\hat{\mathbf{b}}$ is the vector of estimated regression coefficients, **X** is the design matrix obtained when specifying the factor values in the matrix design and **y** is the vector of the response.

Once the regression coefficients have been estimated, the multiple linear regression models can be estimated by

$$\hat{\mathbf{y}} = \mathbf{X}\hat{\mathbf{b}} \qquad \text{(Eq. 3)}$$

where $\hat{\mathbf{y}}$ is a vector of responses predicted by the fitted model, **X** is the design matrix and $\hat{\mathbf{b}}$ is the vector of estimated regression coefficients.

The predicted values of the responses ($\hat{\mathbf{y}}$) can be used to compute the residuals ($\mathbf{f} = \mathbf{y} - \hat{\mathbf{y}}$), which are used in various diagnostic tools described in the diagnostics section.

Once an MLR model has been created, different tests can be performed to assess its validity. For instance, the significance of the regression model can be evaluated (to verify that there is a statistically meaningful relationship between at least one factor and response) using the ANOVA F-test, in which the ratio of the MLR regression sums of squares and the sums of squares for the residuals are computed. T-tests are often used to determine the statistical significance of individual factors. One thing to keep in mind is that the residuals must be normally distributed. It should also be noted that MLR techniques functions

badly if there is high collinearity between factors or if the number of observations is lower than the number of factors. This is because in the MLR solution, the pseudoinverse of ($\mathbf{X}^T\mathbf{X}$) becomes rank-deficient and the solution is undefined.

1.5.3 Principal component analysis (PCA)

Principal component analysis (PCA) is the workhorse technique for multivariate data analysis and is often used as a first step for identifying patterns and groups in large data sets. It is an unsupervised multivariate technique that is appropriate for analyzing spectroscopic collinear data such as NIR data sets. PCA was introduced by Pearson (1901) and has later been reworked by others, using algorithms such as non-iterative partial least squares (NIPALS) (Wold, 1966) and singular value decomposition (SVD) (Golub & Reinsch, 1970). Regardless of which algorithm is used, PCA compresses multi-dimensional data onto a few low-dimensional planes using sets of bilinear functions called principal components (PCs). The objective of the PC placement is to capture as much variation as possible in each PC. The PCs are orthogonal and ranked according to the amount of variance they explain relative to the last and normalized PC. Mathematically, PCA is defined as shown below:

$$\mathbf{X} = \mathbf{T}\mathbf{P}^T + \mathbf{E} \qquad \text{(Eq.4)}$$

where $\mathbf{X}$ is the raw data matrix (often mean-centred) with a size of (I x J), $\mathbf{T}$ (I x A) is a matrix of score vectors, A is the number of PCs, $\mathbf{P}$ (J x A) is the matrix of loading vectors, and $\mathbf{E}$ (I x J) is the residual matrix.

In order to obtain the score vectors $\mathbf{T}$, the sample points (observations) are projected orthogonally onto each principal component. By studying the score-plot, relationships and associations between observations can be found. By analysing the loading vectors, which are the weights that the original variables had when the PC was calculated, correlations between variables can be identified. A common practise is to study the scores and loadings in conjunction in a bi-plot, as was done in Paper II This facilitates the identification of specific variables that strongly influence individual and group score values for specific PCs.

1.5.4 Partial least squares (PLS) regression

The most commonly used method used for multivariate calibration is partial least squares (PLS) regression. PLS was developed by Herman Wold (1966; 1975) and is an iterative method for relating a variable matrix ($\mathbf{X}$) to a response vector or matrix ($\mathbf{y}$ or $\mathbf{Y}$). In PLS, the algorithm models both $\mathbf{X}$ and $\mathbf{Y}$

alternately and thereby maximizes the covariance in both matrices. The general equation of PLS is**:**

$$\mathbf{y}=\mathbf{X}\mathbf{b}_{pls}+\mathbf{f} \qquad \text{(Eq.5)}$$

where **y** is a vector of responses, **X** is the matrix of variables for the observations, **b** is the vector of computed PLS coefficients and **f** is the vector of residuals.

In many cases, the aim of constructing multivariate calibration models using methods such as PLS is to predict the properties of uncharacterized samples. The predictive ability of a PLS calibration model is commonly evaluated by dividing the sample set into a calibration set, which is used to construct the model, and a test set, which is used to test its predictive capability. Typically, two thirds of the samples are used for calibration and the remaining third comprise the test set. Another common practise is to use cross validation to evaluate the calibrated model's ability to predict new samples. Examples of commonly used cross validation procedures include leave-one-out (used in Paper I) or Venetian blinds, whereby one or more samples are left out during the calibration process and predicted by the model. This process is repeated with different samples being excluded during calibration until all of the samples have been excluded once.

When constructing PLS models, it is important to consider the number of PLS components that are used. If the number of components is too small, the model is under-fitted and a large amount of predictive variation may be un-modelled, resulting in worse predictions than could have been made with better modelling. If too many PLS components are used, noise is likely to be included in the model, again worsening its predictive capabilities. The appropriate number of PLS components for the calibration models developed in Paper I was determined by considering the first local minima in the root mean square error of prediction (RMSEP). If the minima were found in the first or second component, the second minima were used to avoid under-fitting.

1.5.5 Diagnostics

The concept of diagnostics is important when considering the usefulness and accuracy of constructed PLS calibration models and MLR models. The diagnostics used in Paper I are mostly based on the vector of residuals from the test set, while the diagnostics used for the MLR models presented in Papers II-V are mainly based on the vector of residuals from cross validation.

Listed below are the diagnostics used in Paper I. The coefficient of determination (Q^2) describes the amount of variation explained in the test set

$$Q^2 = 1-\mathbf{f}_t^T\mathbf{f}_t(\mathbf{y}_t^T\mathbf{y}_t)^{-1} \quad \text{(Eq. 6)}$$

where $\mathbf{f}_t^T\mathbf{f}_t$ is the sum of squares for the residual vector from the validation of the test set and $(\mathbf{y}_t^T\mathbf{y}_t)$ is the sum of squares for the mean-centered response ($\mathbf{y}$) of the observations in the test set.

The prediction error in the calibration models was evaluated by calculating the root mean square error of prediction (RMSEP) according to Eq. 7.

$$RMSEP = [\mathbf{f}_t^T\mathbf{f}_t J^{-1}]^{1/2} \quad \text{(Eq.7)}$$

where $\mathbf{f}_t^T\mathbf{f}_t$ is the sum of squares for the residual vector of the test set and J is the number of observations in the test set.

Another useful diagnostic tool in the evaluation of calibration models is bias; if the randomly chosen samples of the test set are non-representative, they will have a large bias. Bias was calculated according to Eq. 8.

$$Bias = \mathbf{1}^T\mathbf{f}_t J^{-1} \quad \text{(Eq. 8)}$$

where $\mathbf{1}$ is a vector of ones ($1 \times J$), $\mathbf{f}_t$ is the vector of residuals ($J \times 1$) from the test set, and J is the number of observations in the test set.

When constructing calibration models it is often useful to relate the prediction errors to the numerical span of the samples of the model. To this end, Williams and Sobering (1993) proposed the concept of ratio of performance to deviation (RPD), in which the standard deviation of the response vector $\mathbf{y}$ is divided by the prediction error (RMSEP) as shown in Eq.9.

$$RPD = [\mathbf{y}_t^T\mathbf{y}_t(J-1)^{-1}]^{1/2}[\mathbf{f}_t^T\mathbf{f}_t J^{-1}]^{-1/2} \quad \text{(Eq. 9)}$$

where $\mathbf{y}_t^T\mathbf{y}_t$ is the sum of squares for the mean-centred response ($\mathbf{y}$) of the test set, J is the number of observations in the test set and $\mathbf{f}_t^T\mathbf{f}_t$ is the sum of squares for the residual vector of the test set.

An additional diagnostic tool was used in Paper I which also relates the prediction error (RMSEP) to the numerical span of the model. This diagnostic tool is the range error ratio (RER), which is calculated using Eq. 10

$$RER = [y_{max}-y_{min}][\mathbf{f}_t^T\mathbf{f}_t J^{-1}]^{-1/2} \quad \text{(Eq. 10)}$$

where y_{max} and y_{min} are the maximum and minimum response values in the test set, $\mathbf{f}_t^T\mathbf{f}_t$ is the sum of squares for the residual vector of the test set, and J is the number of observations in the test set.

The diagnostic tools used for MLR modelling in the designed experiments described in Papers II – V were based on the residuals between the observed (y_{obs}) and predicted (y_{pred}) responses for each run. Parameters that were found to be non-significant or without significant 2-way interactions or squared interactions were excluded from the modelling. The coefficient of determination (Q^2), i.e. the amount of response variance predicted by the specific model, obtained by cross-validation was calculated in a slightly different way to that used in the PLS calibration modelling, using Eq. 11.

$$Q^2 = 1-\mathbf{1}(\mathbf{1}^T-\mathbf{h})^{-1}(\mathbf{f}^T\mathbf{f})(\mathbf{y}_c{}^T\mathbf{y}_c)^{-1} \quad \text{(Eq. 11)}$$

where **1** is a vector of ones (dimension of Nx1), **f** is the vector of residuals, **h** is the diagonal elements of the Hat matrix (calculated as $\mathbf{X}(\mathbf{X}^T\mathbf{X})^{-1}\mathbf{X}^T$ where the matrix **X** is the coded parameters and interactions for each observation in the calibration set) and $\mathbf{y}_c$ is a vector of the mean centered responses.

To further estimate the predictive capabilities of the constructed MLR models, the residual standard deviation (RSD) was calculated using Eq. 12.

$$RSD = [(\mathbf{f}^T\mathbf{f})(N-p)^{-1}]^{1/2} \quad \text{(Eq. 12)}$$

where **f** is the vector of residuals, the scalar N is the number of observations and p is the degrees of freedom used in the models.

In Paper V, the root mean square error of cross validation (RMSECV) was used as a measure of model quality and RMSECV was computed in a similar way to RSD as shown in Eq. 13.

$$RMSECV = [(\mathbf{f}^T\mathbf{f})N^{-1}]^{1/2} \quad \text{(Eq. 13)}$$

where **f** is the vector of residuals and the scalar N is the number of observations in the models.

Additionally, in Papers II-V, the coefficient of determination (R^2 & R^2_{adj}), which describes the amount of variation explained by the model, was calculated similarly to Q^2 but the vector of residuals was based on the observations in the MLR model rather than the predicted ones. R^2_{adj} was computed similarly but on the basis of the mean squares instead of sums of squares. This enabled comparisons between models with different numbers of

factors and is also important to consider when determining the appropriate numbers of factors in the model.

Finally, the condition number is important to consider when designing experiments because it reflects the orthogonality of the design. The condition number was calculated using the extended design matrix **X,** and is the ratio of the largest to the smallest singular values of **X,** which are often calculated as the eigenvalues of $\mathbf{X}^T\mathbf{X}$ (Eriksson *et al.*, 2008). The extended design matrix is constructed by specifying the factor values used in the design and subsequently scaled and centered and extended to the specific MLR model. A condition number smaller than 3 indicates a good model design while a value above 6 indicates a bad design (Eriksson *et al.*, 2008).

1.6 Objectives

The overall objective for the research that constitutes the backbone of this thesis was to develop methods for characterization and to generate new knowledge and understanding of the parameters that affect the densification of carbonized lignocellulosic biomass.

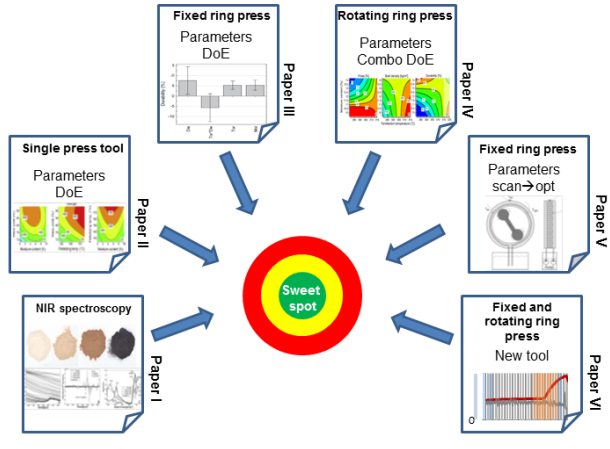

Figure 5. Representation of the papers included in the thesis and the targeted "sweet spot", which corresponds to the generation of new knowledge relating to the characterization and densification of carbonized biomass.

Specific objectives were to

- Investigate the scope for using NIR spectroscopy as a tool to predict the major properties of carbonized biomass samples (Paper I), and to determine whether Py-GC/MS can be used to characterise changes in torrefied materials (Paper IV).

- Study key torrefaction and pelletization parameters in a single pellet press tool by mapping their combined effects on pellet quality and process energy consumption (Paper II), and evaluate the usefulness of bench-scale data in pilot scale applications.
- Conduct a DoE in which process settings and conditions are varied systematically and the influence of torrefaction temperature, torrefaction time, sieve size, moisture content, press channel length, die temperature and pellet temperature on the pellet quality are evaluated and analysed to identify complementary combinations of torrefaction and pelletization conditions (Paper III-V).
- Study and develop new concepts for controlling feed layer formation and utilizing the increased flowability of torrefied particles in feeding devices (Paper V and VI).

2 Materials and methods

Table 1 and *2* summarize the materials, methods and instruments, multivariate statistical tools, and software used in the research presented in Papers I-VI.

Table 1. Overview of materials, analytical methods and instruments, and densification equipment used in the work reported in Papers I-VI. Paper I focuses on the characterization of thermally treated biomass using spectroscopic techniques, Papers II-VI focus on densification, and Papers III, IV and VI deal specifically with the pelletization of torrefied woody biomass.

Studies based on:	Paper					
	I	II	III	IV	V	VI
Materials						
Pine, spruce, reed canary grass	x					
Spruce (shredded 4-8 mm)		x	x			
Pine (chips)				x		
Reed canary grass					x	
Forest residues and willow (chips)						x
Facilities and analytical methods						
Bench scale torrefaction reactor	x	x				
Pilot scale torrefaction reactor			x	x		x
Single pellet press tool		x				
SPC pellet press (fixed die)					x	x
Bühler pellet press (rotating die)			x	x		x
Chemical analysis (C, H, O, N, S, ash content, volatile matter)	x	x	x	x		
FT-IR and NIR spectroscopy	x					
Py-GC/MS				x		
Pellet quality (moisture, strength, durability, bulk density, c_v, energy consumption etc.)		x	x	x	x	x

Table 2. Multivariate methods and software used in Papers I-VI.

Studies based on:	Paper					
	I	II	III	IV	V	VI
Modelling						
MLR		x	x	x	x	
PCA	x	x		x		
PLS	x					
Software						
MODDE (experimental design)		x	x	x	x	
Matlab	x					x
PLS Toolbox	x	x		x		
SIMCA	x	x		x		

2.1 Biomaterials

The experimental work presented in this thesis used biomaterials derived from both the agricultural and forestry sectors. Reed canary grass (*Phalaris arundinacea* L.) was used as a model for rhizomatous and energy grasses, while woody materials were represented by Norway spruce (*Picea abies* Karst. (L.)), Scots pine (*Pinus sylvestris* L.), willow (*Salix viminalis* L.), and forest residues including branches, bark and needles with a mix of Scots pine (17%), Norway spruce (69%) and deciduous trees (14%).

2.2 Thermal pretreatments

In the study described in Paper I, a total of 58 samples were treated at temperatures ranging from 105 °C for drying of raw material up to 850 °C for the solid residues of gasification. The torrefaction of Norway spruce chips and pellets of reed canary grass was performed in a pilot scale continuous torrefaction unit at the Biofuel Technology Center of the Swedish University of Agricultural Science in Umeå, Sweden, at temperatures between 240 and 300 °C, with residence times of 8 to 25 minutes. One charcoal sample was collected from a commercial plant (Vindelkol, Vindeln, Sweden) where wood pieces of 5 to 20 cm from dried lumber were pyrolysed for 8 to 14 hours at a temperature of about 450 °C over the last two hours. This sample mainly contained wood from Norway spruce but also some from Scots pine. Other biochar samples from Norway spruce stem wood were prepared in a drop-tube

reactor consisting of an electrically heated ceramic tube. These samples were treated at 350 to 600 °C for 4 to 40 minutes in an oxygen-free environment. Samples of solid gasification residues derived from reed canary grass and Norway spruce, which had been heated at about 850 °C with a residence time of 4 seconds, were collected from the pilot gasifier at the SP Energy Technology Center, Piteå, Sweden.

For the single pellet study of Paper II, samples of Norway spruce biomass were torrefied under five different sets of conditions. The torrefaction was performed in a bench scale torrefaction unit consisting of a stainless steel box, with a volume of about 1 liter (1), and fittings for gas inlet and outlet. The in-house-built reactor was placed in a programmable muffle furnace (Carbolite furnaces, Bamford, Sheffield, England) and flushed with nitrogen at a rate of 0.5 l $(min)^{-1}$ during torrefaction.

For temperature monitoring, a thermocouple was placed in the middle of the reactor. To reduce the risk of creating a temperature gradient in the sample resulting from a temperature overshoot in the furnace that would produce high temperatures at the reactor surface, the heating was controlled by a thermocouple in the furnace rather than the thermocouple in the reactor. Torrefaction was performed at 5 different temperatures between 250 and 300 °C for one hour. Before torrefaction, the samples (each of which had an initial weight of around 130 g) were dried at 105 °C for 16 hours. The torrefaction time of 1 hour was defined as having started once the reactor reached a steady state at its pre-set temperature.

The torrefied spruce material examined in Paper III was produced in a pilot scale torrefaction plant (20 kg h^{-1}) designed and constructed in a collaboration between Umeå University, the Swedish University of Agricultural Sciences and BioEndev. It achieves torrefaction via a continuous process performed in a rotating drum heated by electrical heaters, and is described in detail by Strandberg *et al.* (2015). The materials were torrefied at 270 and 300 °C for 16.5 min.

For Papers IV and VI, pine biomass, forest residues, and willow were torrefied in the second generation torrefaction reactor (200 kg h^{-1}) in a collaboration between Umeå Universitet and Bioendev. The torrefaction pilot plant is described in detail by Lindh *et al.* (2016). The continuous torrefaction unit features a pre-heated rotary drum (220 °C) in which the raw biomass is pre-treated before passing into an auger screw torrefaction reactor where it is heated to the desired temperature (which is measured with an IR-pyrometer). The reactor is operated at a small negative pressure (0.1-0.15 mbar) with an inert atmosphere. Paper IV examined torrefied pine wood prepared at temperatures of 291-315 °C and residence times of 6-12 min. In total, 12 tons

of torrefied material were produced. The willow and forest residues used in Paper VI were torrefied at 308 °C for 9 min. Before torrefaction, the materials were dried in a low temperature (about 40 °C) flat bed dryer to a moisture content of 4-8 %.

2.2.1 Properties of thermally treated materials

The samples of torrefied and reference biomass were analysed to determine their calorific value and contents of ash, volatile matter, fixed carbon, carbon (C), hydrogen (H), oxygen (O; calculated), nitrogen (N) and sulphur (S) (wt%, dry basis) according to European standard methods (EN 14774-1:2009; EN 14775:2009; EN 14918:2009; EN 15104:2011; EN 15148:2009). Having determined the contents of C, H, O, N, S and ash, H/C and O/C atomic ratios were calculated. The samples' gross calorific values (P_{GCV}) were also estimated using the following formula (Gaur & Reed, 1995):

$$P_{GCV} = 0.3491\times C + 1.1783\times H - 0.1034\times O - 0.015\times N + 0.1005\times S - 0.0211\times ash \quad \text{(Eq.14)}$$

Gross calorific values calculated in this way can be biased; according to the pellet handbook (Obernberger & Thek, 2010), this method overestimates the gross calorific value by 1.8% on average. Mass yields were also recorded for most of the samples as the remaining dry mass of the thermally treated sample as a percentage of its untreated dry mass.

2.3 Grinding

The grinding of material used in pilot scale pelletization (Paper III-VI) was performed in a hammer mill (Vertica Hammer Mill DFZK-1, Bühler AG, Uzwil, Switzerland) with screen sizes from 4-6 mm. The round bales of reed canary grass used in Paper V were shredded before grinding in a single shaft shredder (Lindner Micromat 2000, Lindner–Recyclingtech GmbH, Spittal, Austria) with a 15 mm screen size.

For the single pellet trials discussed in Paper II, the materials were grinded in a knife mill (Retsch SM2000, Retsch, Germany) over a 6 mm sieve. The same knife mill was used to prepare the materials for the NIR and FT-IR spectroscopy experiments in Paper I as well as for the drying experiments in Paper VI but this time over a 1 mm sieve. For FT-IR, the samples were further manually ground with KBr (infrared spectroscopy grade, Fisher Scientific, UK) in an agate mortar; the KBr was added as a background.

The determination of grinding energy in Paper IV was performed using a laboratory mill (Retsch ZM-1, Haan, Germany) with a 0.5 mm sieve.

For the Py-GC/MS analysis, the pellet samples were dried for 24 hours at 105 °C before being ball milled for 2 minutes at 30 Hz in 10 ml stainless steel containers with one 7 mm stainless steel ball (Mill, MM400, Retsch Germany).

2.4 NIR and FT-IR characterization

NIR spectra were acquired with a Perten spectrometer (DA 7250 NIR analyzer, Perten Instruments, Hägersten, Sweden) using a small volume mirror cup exposing a surface area of around 20 cm^2. The samples had volumes of around 11 ml, or masses of around 1.5 to 5.2 g depending on their density. Triplicate samples of each material to be analyzed were scanned, and average reflectance spectra of 50 scans at every wave length from 950 to 1650 nm were recorded, resulting in a total of 58 × 3 spectra with 701 data points. The data were converted into absorbance values before being used to model the relationships between the measured variables and the spectra.

As a complement to the NIR spectra, which featured weak overlapping peaks and broad bands due to overtone vibrations, IR spectroscopy was also used to acquire absorption peaks reflecting fundamental vibrations in Paper I. A Bruker IFS 66 v/S spectrometer was used, with the samples held under vacuum (400 Pa), and a standard DTGS (deuterated triglycine sulfate) detector was used to collect their FT-IR (Fourier transform infrared) reflectance spectra within the wavelength range of 400-5200 cm^{-1}.

2.5 Pelletization

In Papers II-IV and VI, pelletization was combined with a foregoing torrefaction step. *Table 3* lists the torrefied materials used and the conditions applied in their pelletization.

Table 3. Set points in the different pelletizations (Papers II-VI).

Paper	Torrefied temp	Sieve size	Moisture content	Press type*	Channel length	Steam	Die temp
	°C	mm	%		mm	kg h^{-1}	°C
II	250-300	0.5-2	0-10	single	not actual	0	125-180
III	270, 300	6	11-15	rrd	35	0	60-105
IV	291-315	4-6	10-14	rrd	25, 30	0	uncontrolled
V	raw	6	12-16	srd	52.5	0-6	30-65
VI	308	6	9	srd, rrd	50, 52.5	0	30-85

* rrd: rotating ring die (Bühler); srd: stationary ring die (SPC)

For Paper II, pelletization was performed in a single pellet press while for Papers III and IV it was done with a pilot scale ring die. This pellet mill - a Bühler DPCB unit (Bühler AG, Uzwil, Switzerland) - had a rotating die and a set of fixed but free-rolling press rolls. Paper VI describes the pelletization in both the previously mentioned Bühler rotating ring die pellet mill and an SPC PP300 compact (Sweden Power Chippers, Borås, Sweden) pellet mill with fixed die and free rolling rollers. In the latter case, the two rollers were assembled as a pair and the whole set was rotated. The fixed SPC die was equipped with a cooling device, and the pellet mill was equipped with a steam generator and a cascade mixer to mix steam homogeneously in to the material. In Paper V, reed canary grass was pelletized in the SPC pellet mill, and the steam generator and cascade mixer were used together with the cooling device.

The single pellet press pelletization described in Paper II was performed at the Danish Technological Institute using an in-house manufactured press unit (Holm *et al.*, 2007; Shang *et al.*, 2012; Stelte *et al.*, 2013). The die was made of stainless steel and equipped with heaters and thermocouples for control of the die temperature. The press unit was used together with a test system (AGX, Shimadzu, Japan) with a 200 kN load cell. The torrefied and grinded material was separated into two different fractions according to the particles' diameter: small (i.e. < 0.5 mm) and big (0.5 mm – 2 mm). Thereafter the samples were adjusted to five different moisture contents between 0 and 10% and then packed and sealed in gas-tight plastic bags for equilibration over one week before pelletizing. A mass of 750 mg ± 5 mg of material was fed into the die and compressed in one step at a rate of 100 mm min^{-1} until a maximum pressure of 300 MPa was reached; this pressure was then maintained for 5 seconds. Thereafter, the stop piston was removed and the pellet was pressed out of the press channel with the same speed as it was compressed. The test system recorded the force and distance to enable calculation of the response variables W_{comp}, F_{max} and W_{fric}. Other parameters measured and recorded were the pellets' strength, weight, length, diameter and density. In total, 29 experiments were performed according to a fractional factorial experimental design with four parameters.

The experiments of Paper III and Paper IV used a Bühler press with rotating die. The experiments of Paper III were performed at two levels of torrefaction (300 °C for 16.5 min and 270 °C for 16.5 min) and moisture content (11 and 15%). Three of these runs were repeated as replicates. During each run, samples were collected 3 times over a period of 2 minutes. The samples were analyzed for moisture content, fines during production, bulk density, durability and production rate. These results were used as responses in the data analysis. The die temperature was measured with a fixed IR sensor (Optris CT LT 15:1,

Optris GmbH, Berlin, Germany) and the pellets' temperature was recorded in three of the seven runs using a handheld IR sensor (Optris CT laser 75:1, Optris GmbH, Berlin , Germany) directed towards the pellets immediately as they left the die.

In Paper IV, each pelletizing experiment consumed around 400 kg of torrefied pine wood. A total of 19 individual experiments were performed in a combined experimental design evaluating the impact of torrefaction (torrefaction temperature and retention time) and densification (sieve size, moisture content, press channel length and pellet temperature) variables on responses relating to the pellets' handling and storage properties. After grinding, the moisture content of the torrefied material was adjusted (to values between 10 and 14%) in a screw mixer with load cells where the whole batch could be adjusted at the same time in order to ensure that the moisture content remained consistent throughout the experiment. The moisture content-adjusted material was then left to equilibrate for 16 hours before pelletization, which was performed using two different press channel lengths of 25 and 30 mm.

Triplicate samples were collected from each experimental run once the pellet production conditions had stabilized. The sampling period was 1-3 minutes, depending on the fines content of the produced pellets. This was done to ensure that enough pellets were sampled for the planned analyses. The collected pellets were stored in open containers, then weighed and cooled before being sealed in airtight plastic bags until further sub-sampling (see *Figure 6*).

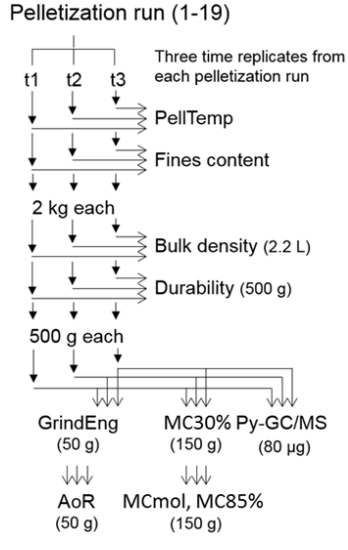

Figure 6. Overview of the sampling process used in Paper IV (from Paper IV).

This sampling was done to characterize the pellets according to their fines content, bulk density, mechanical durability, moisture content, energy required for grinding, and angle of repose. Chemical markers for cell wall decomposition during torrefaction was analysed by Py-GC/MS. During pelletization, the pellet mill's motor power was recorded along with the pellet and die temperatures.

The experimental work for Paper V was performed using an SPC pellet mill with a fixed die together with a cooling device that circulates cool water inside the die and thereby cools it without adding water to the pelletized material. Over measurement periods of two minutes, pellets were sampled and data were gathered from the pellet machine's control unit for further analysis. Die and raw material temperatures were measured with a Type-K thermocouple, along with the cooling system's temperature. The pellet mill motor's current was measured continuously (1 Hz) and the signals from temperature and current were collected by a logger system (PC-logger 3100i, Intab Interface-teknik AB, Stenkullen, Sweden). Pellet quality responses such as the fines content, durability, bulk density and moisture content were analyzed by standardized methods (EN 14774-1:2009; EN 15103:2009; EN 15210-1:2009). Fines during production were determined according to the sieving procedure described in the standard for durability.

Paper VI explored the use of cooling as a way of maintaining the pellets' moisture content at a level that would allow pellet production to remain in a steady state. In some of these experiments, the SPC pellet mill was used together with a cooling device that circulates cool water in the die and thus cools it without adding water to the pelletized material. In other experiments, the Bühler pellet mill was used and cold water was added directly to the material inside the die. As the temperature rose, more water was added to prevent the temperature from rising beyond the desired level. The pellets obtained using both procedures were characterized with respect to their fines content, bulk density, mechanical durability, moisture content and energy consumption.

The torrefied materials used in Paper VI and the raw materials they were made of were also analyzed for drying rate. The drying rate analysis were executed in a drying balance (HB43, Mettler Toledo, Greifensee, Switzerland) with a halogen heating source at a temperature of 105 °C and a 3 digit scale where the weight changes were logged with a frequenzy of 1 Hz.

2.6 Py-GC/MS

Samples (80±5 µg) of powder from torrefied and pelletized materials (weighed on an XP6 microbalance, Mettler-Toledo, Switzerland) were placed in autosampler cups (Eco-Cup SF, Frontier Labs, Japan) and loaded into the pyrolyser (PY 2020iD and AS1020E, Frontier Labs, Japan), which was connected to the injector of a GC/MS instrument (7890A-5975C, Agilent Technologies AB, Sweden). The sample was then flash pyrolysed at 450 °C, after which the degradation products were split 16:1 at 320 °C and then sent to the GC and separated on a column (Ultra Alloy^{+}-5,30m, 0.25mm inner diameter, 0.25 µm film, Frontier Labs, Japan). The column's temperature was initially 60 °C and was raised by 16 °C/min until it reached 320 °C, at which value it was held for 3 minutes. Analytes eluting from the column were transferred at 280 °C to the ion source (70 eV, 280˚C) and then separated and detected in full scan mode (18-250 m/z). Processing of the raw data and peak picking were performed using multivariate curve resolution by alternate regression (MCR-AR) as described by Gerber *et al.* (2012). Peak identification was performed manually using NIST libraries and pyrolysis-specific libraries (Faix *et al.*, 1990; Faix *et al.*, 1991) to assign compounds to lignin- and carbohydrate-specific degradation groups. Three compounds were used to model the extent of degradation of different cell wall components: furfural, levoglucosan and guaiacol, which primarily originate from hemicelluloses, cellulose and lignin, respectively. The peak areas of each detected analyte were normalized against the total area of the chromatogram.

2.7 Modelling and diagnostics

In Paper I, II and IV an overview of the data was done by PCA. In Paper I PLS regression based on mean centered values of NIR spectra and reference variables was used for the calibration modelling. In Paper II-V the modeling of the experimental designs was carried out by MLR.

The diagnostic statistics used was based on the residuals between observed and predicted values in a test set. These diagnostics were: root mean square error of cross-validation (RMSECV), root mean error in prediction (RMSEP), coefficient of multiple determination (Q^2), ratio of performance to deviation (RPD), range error ratio (RER) and residual standard deviation (RSD). In combination with MLR modeling condition number was also used.

3 Results and discussion

An overview of the materials used in this thesis is presented in *Figure* 7, which shows the range of O/C and H/C ratios that they span, and their gross calorific values, which were estimated from their theoretical C, H and O contents using the expression described by Gaur and Reed (1995) (Eq.14). The materials were assumed to contain no N and S (neither of which are very abundant in wood or overwintered straw) or ash. That is to say, each material was assumed to consist exclusively of C, H, and O. The results presented in Paper I indicated that for the observed results (circles in *Figure 7*), GCV values computed based on the materials' C, H and O contents as determined by an NIR calibration model underestimated their energy content by 0.31% on average, within a range of 18.8–34.0 kJ g^{-1}. Thus, the colouring of *Figure 7* gives good estimates of the GCV that can be expected at different H/C and O/C ratios, at least within the range of observed values. The samples examined in Paper I ranged from untreated materials to thermally treated materials with mass yields of about 20 %. The mass yields of the materials considered in Papers II-III and VI ranged from 71 % to 93 %, with untreated materials being used as references.

The response surface in *Figure 7* clearly shows that the gross calorific value decreases if the H/C ratio decreases while the O/C ratio remains constant, and that the opposite occurs if the O/C ratio decreases while the H/C ratio remains constant. The diagram indicates that elemental dehydration occurs as the degree of torrefaction increases, i.e. two H atoms and one O atom are lost relative to the content of C atoms. The simultaneous loss of H and O, and the relative increase in the abundance of C explains why the gross calorific value increases when biomass is torrefied. The empirical formula of biomass was estimated to be $CH_{1.5}O_{0.6}$ on the basis of an analysis of 715 samples published by Tao *et al.* (2012b); if all of the oxygen in a material with this composition were released as H_2O, the residual material would have an empirical formula of

C $H_{0.3}$. This corresponds to an atomic H/C ratio of 0.3, which is close to the offset of the trend line in *Figure 7* when the O/C ratio is zero.

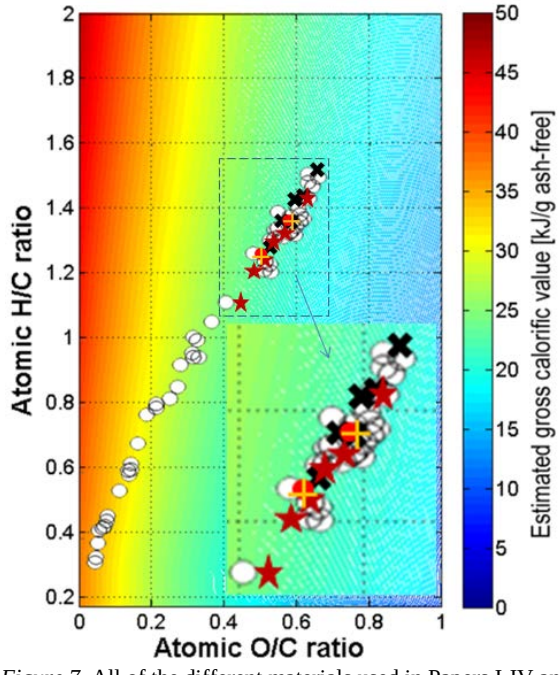

Figure 7. All of the different materials used in Papers I-IV and VI are compiled in this figure. The contour plot shows the atomic H/C and O/C ratios of each material and the corresponding ash-free gross calorific values for carbonised samples as reported in Paper I (open white circle), Paper II (dark red star), Paper III (yellow +), Paper IV (black x) and Paper VI (filled red circle).

As noted in the introduction, biomass is highly heterogeneous in terms of its composition, i.e. its relative content of hemicelluloses, cellulose and lignin (Vassilev *et al.*, 2012). It is generally assumed that thermal treatment reduces this heterogeneity. The different kinds of biomass examined in Paper I all appeared to behave similarly during thermal decomposition, but retained differences in their physicochemical properties that could influence their downstream processing. Therefore, when attempting to optimize the overall outcome of combined torrefaction and pelletization processes, it is important to have analytical and monitoring tools that enable effective process control.

The following sections discuss the results obtained in the individual papers included in this thesis. Paper I deals with the use of NIR spectroscopy as a method for predicting a wide range of variables of interest for process control, focusing particularly on thermal treatments. Paper II describes the use of a single pellet tool to gain knowledge about the compression work done on torrefied biomass during pelletization and the friction that is generated when

using material that has been torrefied to different degrees. The results obtained using this combined bench-scale approach were considered in the following studies. On the basis of the findings described in Papers II-IV, it was concluded that there was a need to better understand the parameters that govern the outcome of the pelletization process in order to more effectively control it and accommodate variation in the physicochemical properties of the feedstock of torrefied biomass. The studies described in Paper V were thus conducted to characterize the processes that cause losses during pellet production due to the breakup of the feed layer between the die and the rollers, and to help develop new ways of improving process control. In Paper VI attempts were done to develop and test new methods to control feed layer formation inside press dies. By improved control of the material´s moisture content at the moment when the feed layer is formed then also the conveying may be improved by utilization of better flowability using surface dry torrefied powders. These two improvements used simultaneously may result in more even pellet production.

3.1 Carbonized materials

The analyses of the carbonized materials used in Paper I revealed a strong correlation between the mass yield (my) of the torrefaction process and the carbon content of the torrefied material, as shown in *Figure 8* (taken from Paper I).

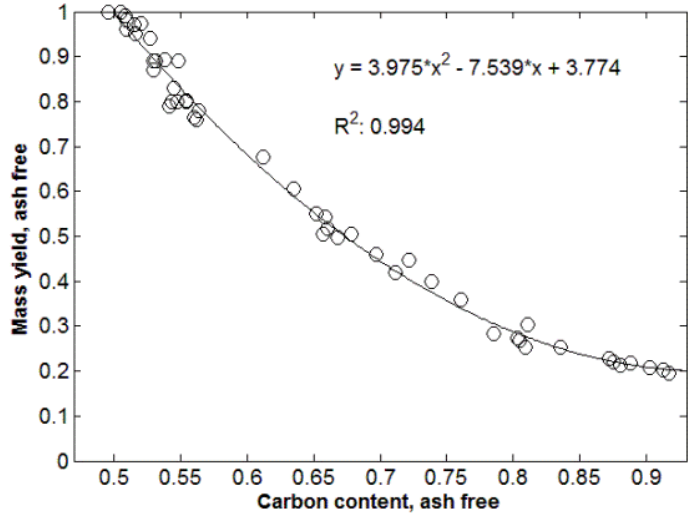

.

Figure 8. Relationship between the mass yield of thermally treated biomass and the carbon content of the resulting material (ash free data).

A 2nd order polynomial curve (Eq. 15) was fitted to the mass yield data, using the carbon content (c) as the independent variable. This explained 99.4 % of the variation in mass yield:

$$my = 3.774 - 7.539c + 3.975c^2 \quad \text{(Eq. 15)}$$

The observed data for the five torrefied materials studied in Paper II were used to validate the polynomial obtained in Paper I. *Table 4* presents the observed and calculated values. The mean average difference between the predicted and measured values was 0.4%, and the average error (root mean squared error) was 0.51 percentage units in mass yield within the interval between 71% and 100%. This relationship between carbon content and mass yield thus seems to be quite robust, at least for torrefied Norway spruce wood.

Table 4. *Observed and calculated mass yields (ash free data).*

C (%)	Mass yield (%) observed	Mass yield (%) predicted
59.1	71.0	71.2
57.1	75.8	76.9
55.8	80.3	80.7
54.3	85.7	85.3
53.0	90.5	89.4
50.6	100.0	97.4

The mass yield of a torrefied biomass is also suggested by Grigiante and Antolini (2015) to state the condition of the torrefied biomaterial when it comes to ultimate analysis, gross calorific value and hydrophobical behavior without considering the pathway regarding torrefaction time and temperature. Strandberg *et al.* (2015) also suggests that torrefaction time and temperature can be interchangeable but only to some extent. MLR models of responses were used to make plots for where in the time and temperature space the preferred values for mass yield, volatile matter, gross calorific value and milling energy were fulfilled. This resulted in a quite large variety of process settings that were interchangeable. When equilibrium moisture content and angle of repose for the torrefied materials were added to the earlier responses the area for the process is decreased. If further responses of interest for the pelletizing process are added such as hemicellulose, cellulose and lignin degradation then this will decrease the interchangeable area, and finally to a single point where all treated materials are unique.

3.2 Spectroscopic characterization

The effects of the carbonization processes studied in Paper I were best described by considering the FT-IR spectral peaks corresponding to specific functional groups in the torrefied material. The samples were sorted into five different groups on the basis of their carbon contents (47-55%, 55–60%, 60–70%, 70–80% and 80-91% carbon, respectively), and average NIR and FT-IR spectra were computed for each group. This revealed that as the degree of carbonization increased, the intensity of absorption for the narrow bands corresponding to C=C, C=O and C–O groups increased, while that of the broad C–H and O–H bands decreased. The reduction in intensity of the O-H bands is particularly interesting because the removal of OH groups would reduce the potential for hydrogen bonding between particles during pelletization.

Calibration models based on the NIR spectra exhibited excellent predictive performance, with Q^2 values exceeding 0.98 for mass yield, volatile matter content, GCV, contents of C and O, and the O/C ratio. This indicates that NIR spectroscopy could be used for fast on-line characterization and for monitoring and control of thermal treatment processes to ensure the production of torrefied material with a consistent quality, which is important for downstream processes such as pelletization. In the case of torrefaction it may be important to regulate the torrefaction temperature and/or residence time to ensure that the variation in the product's H/C and O/C ratios remain within certain limits. Studies by Lestander *et al.* (2009; 2012a) have shown that it is also possible to utilize NIR spectroscopy during pelletization to characterize the ingoing material and adjust the pelletizing parameters based on the collected NIR signals.

3.3 Py-GC/MS

In the Py-GC/MS pyrograms obtained from powder of pellets made of torrefied pine wood (Paper IV) three markers for the degradation of main cell wall components were selected: guaiacol for degradation products derived from lignin, levoglucosan of mainly cellulose, and furfural representing degradation products to some extent from cellulose, but mainly from hemicellulose (Shen *et al.*, 2010; Mante *et al.*, 2014; Zheng *et al.*, 2015). The first principal component (PC1) in the PCA score plot of *Figure 9A* separates the samples by degree of torrefaction (left to right). The corresponding loading plot (*Figure 9B*) shows the parameters and variables responsible for this separation. The used model products to evaluate the degradation of the three main cell wall constituents were clearly separated by torrefaction temperature (TorrTemp), but also by torrefaction time (TorrTime), along PC1 explaining 40.2 % of the

variation in all data. For furfural, its content decreased, but for levoglucosan and guaiacol their content raised with increasing torrefaction degree. The second component (PC2) was influenced by pelletization parameters and responses and showed no influence on these degradation products.

This dependence of TorrTemp and TorrTime was also found in the MLR models whereas other model parameters had no significant influence. Thus, pelletization parameters did not influence the measured amounts of degradation products. One reason for this may be that the observed pellet temperature (46.5-107.5 °C) (Paper IV Table S1) did not introduce any chemical degradation influencing these Py-GC/MS markers.

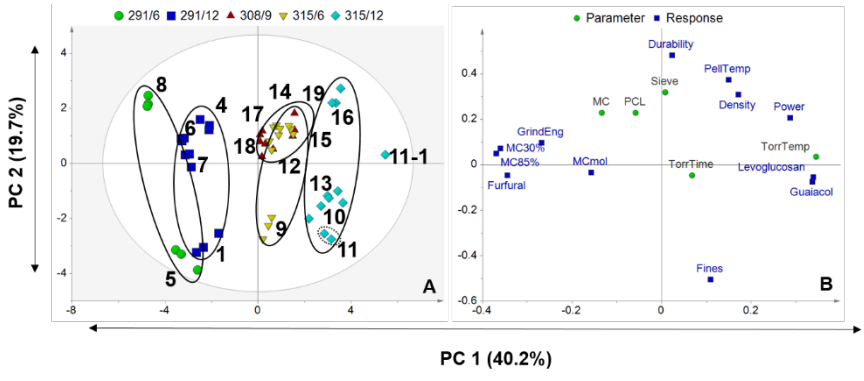

Figure 9. From Paper IV. PCA score plot (A) of observations and loading plot (B) of parameters (circles) and responses (squares) for pelletization runs 1 and 4-19 (Paper IV Table S1). Observations relating to experimental runs conducted using the same torrefaction conditions are shown using the same symbol and color. Here the focus is in the loading plot showing the degradation products: furfural, levoglucosan and guaiacol. Abbreviations a) parameters: Sieve (sieve size), MC (moisture content), TorrTemp (torrefaction temperature), and TorrTime (torrefaction time), PCL (press channel length); b) uncontrollable variable: PellTemp (pellet temperature); c) responses: MC30% and MC85% (moisture content of pellets), MCmol (pellets' water uptake), and GrindEng (grinding energy).

As shown in Figure 9 and by the MLR models in Paper IV, it was found that variation in the properties of torrefied material resulting from changes in the torrefaction temperature and residence time can be characterized by Py-GC/MS using the degradation products furfural, levoglucosan and guaiacol. Given the need to maintain the properties of the torrefied material within a narrow window to facilitate downstream processing (e.g. pelletization), this analytical tool may thus be useful for fine-tuning the effects of changes in the degree of torrefaction. These results follow the pattern observed in earlier torrefaction and pyrolysis studies (Bourgois & Guyonnet, 1988; Sharma *et al.*, 2004; Park *et al.*, 2013; Kim *et al.*, 2014; Wen *et al.*, 2014). Py-GC/MS is of interest as

analytical tool to characterize torrefied lignocellulose and may be of great value as it is less labor intensive than many wet-chemistry protocols. The method is slow in comparison with NIR spectroscopy but provides more detailed chemical information.

3.4 Pelletization

Torrefied biomaterials were pelletized on a range of different scales during the work presented in this thesis. Small scale single-pellets trials in Paper II were performed according to an experimental design that was intended to help define boundaries for later large-scale studies, which used experimental designs involving both pelletizing and torrefaction parameters to evaluate pilot scale pelletization processes.

The only torrefaction factors considered in the single pellet press trials of Paper II were the mass yield of the torrefied raw material. The other factors considered in these studies related to the pelletizing process, and included the particle size, the moisture content of the pelletized material, and the pelletizing temperature. The measured and modeled pelletizing responses were the compression work (W_{comp}), static friction (F_{fric}) and friction work (W_{fric}), as well as five responses relating to pellet quality: pellet strength, weight, length, diameter and density. All responses except W_{fric} and density were influenced by the particle size. Fine particles reduced W_{comp} but increased the pellet strength and slightly increased F_{fric}. A lower degree of torrefaction (i.e. a higher mass yield) and higher pelletizing temperatures improved pellet strength and reduced the energy required for compaction and the particle-to-wall friction. In general, W_{comp}, W_{fric} and F_{fric} declined as the moisture content, mass yield and pelletizing temperature increased; higher pelletizing temperatures enhanced the effects of the moisture content and mass yield.

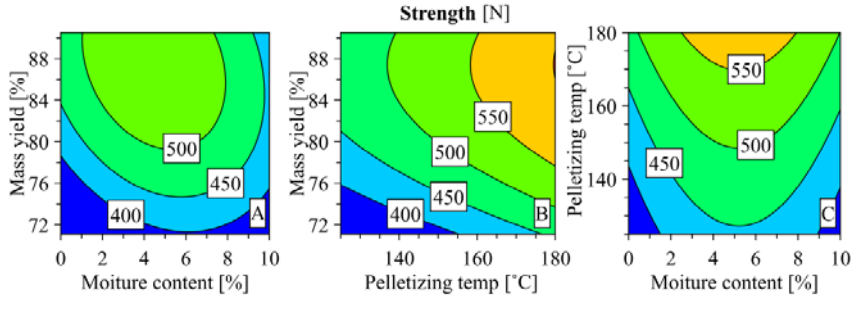

Figure 10. Surface plots showing the influence of mass yield, moisture content and pelletizing temperature on pellet strength (Newtons at breakage). Plots shown with parameters at their intermediate values except for particle size, which was set to small in all plots. From Paper II.

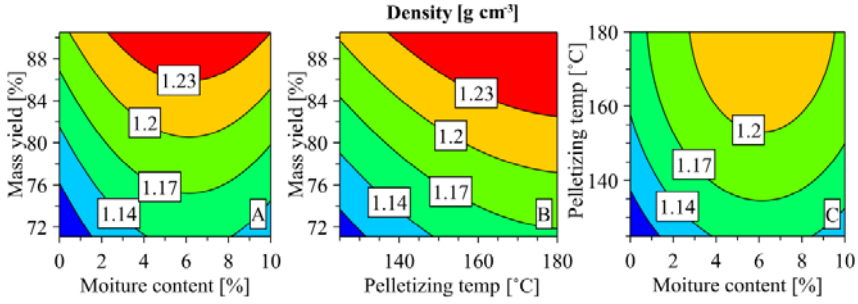

Figure 11. Surface plots showing the influence of mass yield, moisture content and pelletizing temperature on pellet density. Contour plots shown with parameters at their intermediate values except for particle size, which was set to small in all plots.

The contour plots for both strength and pellet density indicate an optimum moisture content of around 5-6 %, with higher pelletizing temperatures and mass yields increasing these responses (see *Figure 10* and *Figure 11*).

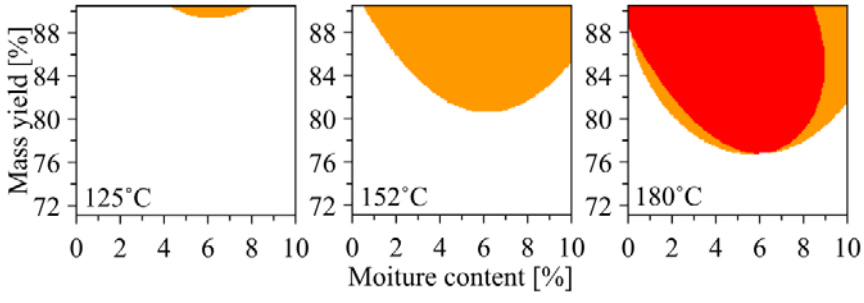

Figure 12. Sweet spot plots at different die temperatures (125, 152 and 180˚C), with criteria of density >1.2 and strength >540 N. The orange area corresponds to densities above 1.2 g cm^{-3} and the red area is the region in which both criteria are satisfied.

A sweet spot plot (*Figure 12*) shows that a pellet with density over 1.2 g cm^{-3} and a strength over 540 N can be achieved with mass yields as low as 79 %. According to Obernberger and Thek (2010), a variation from 1.12 -1.3 g cm^{-3} have been noticed for pellets from untreated wood and that a very rough approximation of the bulk density can be obtained by dividing the particle density by two. The pelletizing temperature at which the criteria for density and strength are both fulfilled in this case is as high as 161 °C, which could be hazardous to maintain in a full scale pellet mill (Shang *et al.*, 2014).

The main conclusion is that there is a rather narrow process window for optimizing pellet quality. The moisture content optimum for strength is around 5-6 %; for comparative purposes, the moisture content in the pilot scale pelletization of torrefied Norwegian spruce reported in Paper III varied

between 11 and 15 %, and in that case there was a positive correlation between moisture content and durability. This indicates that there are important differences between the pelletization methods examined in these two cases.

In the single pellet trials, it is easier to control individual parameters than in pilot scale or full scale pellet mill experiments, where the moisture content at the moment of pelletization can be difficult to monitor. The monitored moisture content will be the moisture content immediately before the raw material enters the pellet mill. In the pellet mill, where the material meets the warm environment of the die and rolls, the material may undergo a degree of drying. The extent of drying will depend on the temperature of the die and also the raw material's ability to retain water. This might be why there is a difference in the optimum moisture content between the single pellet method and pilot scale pelletizing.

In Paper III, torrefied spruce of two different torrefaction degrees was pelletized at a moisture content of 11 and 15 %. The overall practical experience from these runs was that torrefied materials of lower mass yield and higher moisture content generated feeding problems due to blocking and bridging in the feeders. The resulting pellets were of comparable quality to commercial softwood pellets in terms of bulk density but less durable, and the level of fines generated during pelletization was higher than in the production of softwood pellets. Higher moisture contents did not reduce energy consumption or improve pellet quality except for durability, which increased with moisture content.

A full factorial design was used to study the pelletization of torrefied spruce in Paper III. However, due to limitations on the available torrefaction capacity (20 kg h^{-1}), the number of parameters included was limited. Paper IV applied a more comprehensive design in which the design space was expanded to include the torrefaction temperature and time, press channel length, and sieve size as factors. The torrefaction factors time and temperature were varied separately to facilitate independent analysis of their effects. The degree of torrefaction was chosen to be slightly different from the one used in Paper II (71.1-90.5%), ranging from approximately 73 to 85 %. In addition, the moisture contents were slightly lower than those used in Paper III, in the hope that this would minimise the incidence of bridging while the material was fed into the pellet mill. Thus, the moisture content of the initial material ranged from 10 and 14 % to compensate for drying before actual pelletizing. This regards to the lower moisture content optima suggested in Paper II.

The degree of torrefaction and in particular the torrefaction temperature was the parameter with the greatest influence on the pellet quality. Higher degrees of torrefaction yielded material that (i) required less energy when grinded, but

more power to pelletize; and (ii) contained lower quantities of furfural but higher amounts of levoglucosan and guaiacol according to Py-GC/MS analysis. In keeping with previous findings, the set of parameters influencing the pellet quality response variables were quite complex. A general pattern was that a low degree of torrefaction and a high initial moisture content resulted in low production of fines and high durability as well as an acceptably high bulk density. It was thus concluded that one particular corner of the model space offered the best pellet quality, see *Figure 13*.

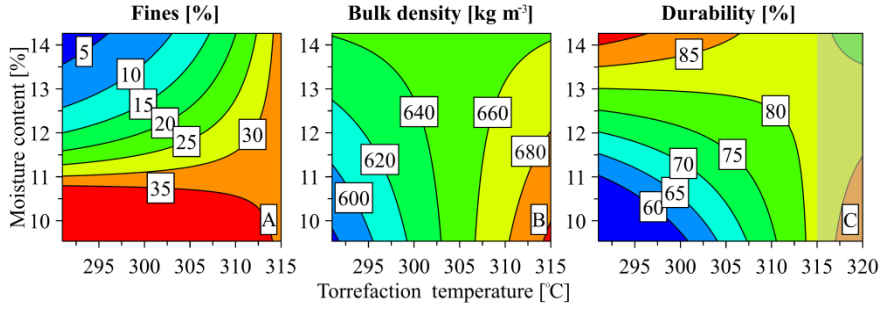

Figure 13. Response plots showing the combined effects of torrefaction temperature and moisture content with a press channel length of 30 mm, pellet temperature of 78°C and torrefaction time of 9 minutes for fines (A), bulk density (B) and durability (C). For durability, the response surface is extended outside the investigated design space to a temperature of 320°C. From Paper IV.

The sieve size parameter had no significant effect on any of the studied responses. However, in the single pellet study of Paper II, all responses except density and weight were influenced by the size of the pelletized material. This might indicate that the difference in size distribution between the materials hammer milled over a sieve 4, 5 or 6 mm was not large enough to make an impact. Torrefied materials are brittle and easy to mill and may thus be more prone to form finer particles independently of the sieve size. In the single pellet trials, the materials were sieved into two totally separate size groups.

Of more academic interest is the finding that there may be a saddle point for fines content and durability just outside the upper torrefaction temperature range, as shown in *Figure 13*c where the response surface is extended outside the investigated design space to 320 °C. To find out if these saddle points are real, the design space should include torrefaction at 320-325 °C for 6-12 minutes with lower initial moisture contents. For future research, it is also suggested the inclusion of smaller (<5 mm) press channel intervals to enable more fine-tuning because there is a close interaction between the degree of torrefaction, moisture content and press channel length.

The reliability of the identification of the high productivity corner is limited by the lack of results corresponding to a press channel length of 25 mm and torrefaction at 291.4 °C for 6 minutes. These set-points were probably lost because the press channel was too short, suggesting that the design space was not optimal for materials of high mass yield. A design spanning press channel lengths of 30-35 mm may thus have been better. Such longer press channels may cause problems in the opposite corner of the design space, where the degree of torrefaction is more severe and known to correlate with the friction. This suggests that the different materials may be too different to be evaluated in the same design. Therefore, in the section on 'Future research' there is a proposal to use fixed channel designs within a single die to scan and match press channel lengths with particular torrefaction degrees using only small amounts of feedstock. *Figure 13* also indicates a strong influence of moisture content for the least torrefied material, but higher moisture contents have been shown to cause problems during conveyance (Paper III).

3.4.1 Die temperature control

Controlling the die temperature offers improved opportunities to control the pelletizing process and potentially to separate the effects of confounded factors. An example of a confounding factor is steam addition, which affects both the moisture content and the temperature of the material. Cooling or heating of the die may partially compensate for the temperature effect of steam. In Paper VI, the die was cooled with a cooling circuit to suppress the drying effect of the material, making it possible to more effectively control the moisture content of the pelletizing material until it was compressed against the die by the rollers.

The loss of feed layer formation, leading to uneven pellet production and an uneven pellet mill motor current can result from an overly low moisture content as a result of drying. This phenomenon may be reinforced by low bulk density and low inner friction (particle-to-particle friction) in the torrefied material, which may cause the feed layer to slip away from the press nip between the die and roll.

In Paper V it is shown that die temperature control is a feasible way to overcome discontinuous pellet production. These disturbances in pellet production were also observed in the preliminary tests conducted to select the press channel lengths to be examined in the study reported in Paper IV. A press channel length of 35 mm was found to produce excessive levels of friction, which is likely to have generated heat to an extent that caused drying of the material and destabilisation of the feed layer. Similar behaviour was observed

during pelletizing of torrefied willow and forest residues, and so the outcome of providing cooling during pelletization was explored in Paper VI.

Larsson *et al.* (2008) introduced the coefficient of variation $c_v = \sigma\mu^{-1}$ as a criterion for characterizing continuous pellet production. Here, σ is the standard deviation and μ is the mean value of the pellet mill motor current during a period of measurement. A value of $c_v < 0.2$ was used to define continuous pellet production. In Paper V, an initial screening study was performed using the raw material moisture content (12-15%), steam addition (0-2 kg h^{-1}) and die temperature (35-65°C) as factors. To achieve a c_v of <0.2 for the optimization experiment, the die temperature was set to 30-45˚C, the raw material moisture content was set to 13-16 % and the steam addition was set to 2, 4 and 6 kg h^{-1}. These values correspond to raw material temperatures of 28-34 °C, 37-42 °C, and 47-52 °C, respectively.

These two steps of the designed experiments showed that the bulk density was highest when the moisture content, die temperature and material temperature were low. At high material temperatures, the bulk density was also high when the moisture content was high. The durability of the produced pellets was > 98 % at low moisture contents when the die temperature was low and at high moisture contents when the die temperature was high. This may indicate that drying occurred inside the die. When the die temperature increased, the drying of the raw material to be pelletized also increased. For materials that are prone to rapid drying, control of die temperature will probably help to maintain a consistent pellet quality. Torrefied materials have greater void volumes than raw biomass (Chen *et al.*, 2014) but fewer water-binding functional groups such as hydroxyl (-OH) (Kymäläinen *et al.*, 2015) and carboxyl (-COOH) (Shoulaifar *et al.*, 2012). Furthermore, torrefied materials have lower EMC values than raw untreated materials (Chen *et al.*, 2014; Kymäläinen *et al.*, 2015), which was also found in Paper IV. Thus, torrefied materials can hold large quantities of water but at the moisture contents of about 10-14% that are typically used in conventional wood pelletization, the water in torrefied wood is less robustly bonded (e.g. by hydrogen bonding) than untreated materials. This is illustrated in *Figure 14* (from Paper VI), which shows that torrefied wood of Salix and forest residues have higher drying rates than untreated wood.

The importance of interactions between water and the pelletizing material depends on the subprocesses occurring, however. Free water will evaporate readily from the material when it is warmed on a die that has been heated by friction. When the material is entering the press nip to form the feed layer, it is important that lateral adhesion of the feed layer can withstand friction generated by the press rollers. At this point, increased moisture contents may

cause the formation of liquid bridges between particles, preventing the feed layer from slipping away from the nip between the roll and die. This phenomenon is discussed in Paper III, where high moisture contents caused problems with bridging when feeding torrefied material.

The drying behaviour shown in *Figure 14* together with the results from Paper V guided the cooling tests described in Paper VI. Cooling could be considered counterproductive given the effects of higher temperatures reported in Papers II-IV. However, the results of the cooling experiments with torrefied forest residues in the SPC pellet mill where cooling was possible without adding water to the material showed that the pellet temperature did indeed decrease as the die temperature was reduced, but the pellets were less strongly cooled than the die. This indicates that cooling of the die mostly affected the material at feed layer formation but before extrusion. However, in Paper VI, raising the die temperature increased the content of fines in the final product, and as a result pellet mill motor current became more variable but this energy consumption decreased with decreasing pellet quality. Thus, in this case, cooling increased the production of fines and reduced the pellets' durability and bulk density. The use of water to cool the rotating die enabled the material to maintain the moisture content necessary for feed layer formation whereas just cooling the press with a fixed die (as in the SPC mill) would probably cause the loss of the feed layer at an earlier stage, as the die temperature increased.

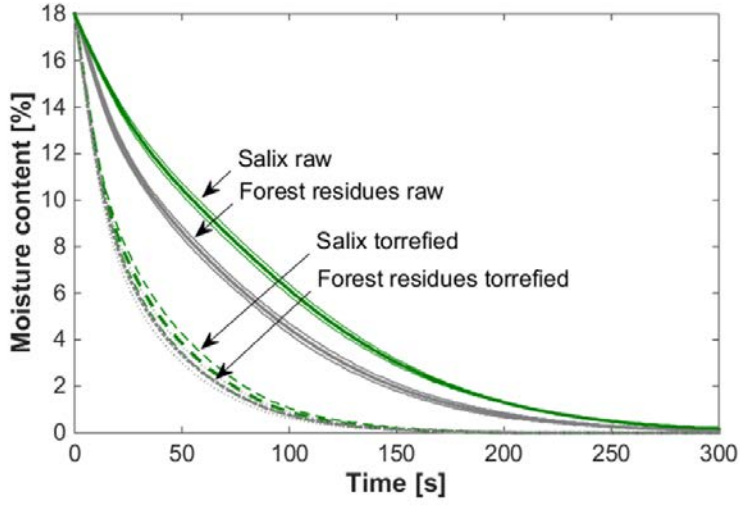

Figure 14. Average drying rates (+/- one standard deviation) of powders from untreated and torrefied wood of Salix and forest residues. From Paper VI.

The problems with feed layer loss when the material dries out together with results from Paper II where the optimal moisture content was around 5 % indicate that the binding mechanisms that dominate during feed layer formation are different to those that are most important in pelletization, when the feed layer apparently requires a higher water content to remain stable.

New innovative tools to cool the pellet-forming material in pellet mills with stationary and rotating dies were developed in Paper V and VI, respectively. The tool for the rotating dies makes it possible to directly inject water into the space inside the die. It was used in the pelletization of torrefied willow as an alternative cooling method to the indirect cooling applied when pelletizing forest residues.

The aim in these tests was to maintain steady pellet production with the ability to increase the degree of applied cooling as required to achieve this goal. The added water promoted the formation of a stable feed layer but also affected the pellet quality. The bulk density decreased as the moisture content increased, which is consistent with previously reported results for white pellet production (Samuelsson *et al.*, 2012).

The overall conclusion from these experiments was that the injection of water could maintain production in a steady state, but the high water flow needed for cooling adversely affected pellet quality by reducing bulk density and durability. Another piece of knowledge relevant to the development of innovative pellet production processes is that direct nozzle injection of water in front of the press nips makes it possible to improve the flow of torrefied particles (especially for material with a dry surface) while simultaneously cooling the feedstock and controlling its moisture content.

4 Conclusions

The main conclusions of this thesis are:

- NIR spectroscopy can be used to predict a broad range of physicochemical properties of thermally treated biomass samples including the elemental composition of their organic components and their contents of energy, volatile matter and fixed carbon. It could thus be useful as a standardized technique for characterizing carbonized lingocellulosic biomass as well as applied on-line to monitor and control processes.
- The chemical variation arising from changes in torrefaction temperature and duration can be detected using Py-GC/MS analysis, indicating that this technique may be used as a fingerprinting tool.
- Studies using a single pellet press tool can provide new insights into the pelletizing properties of torrefied materials such as their mass yield, pelletizing temperature, moisture content, and material size, and the way in which these qualities influence pelletizing responses such as compression and friction work, pellet dimensions and strength. The results of these bench scale studies indicates that there is a narrow window of parameter combinations that can provide acceptable pellet quality when pelletizing torrefied materials in general.
- Pelletizing experiments using both a single pellet press tool and a pilot scale plant using torrefied (270-315˚C, 6-16.5 min) material from soft wood species (Norway spruce and Scots pine) and a hard wood species (*Salix viminalis* L.) indicated that torrefaction increased the energy required for pelletization relative to that for untreated wood, and yielded pellets of comparable bulk density but lower durability.
- Experiments using torrefied Norway spruce and Scots pine wood in a pilot scale mill with a ring die of the type used in industrial pelletization verified the narrowness of the process window for pelletizing torrefied material.

- The DoE space revealed that pellet quality was highest when the initial moisture content was high and the degree of torrefaction was low (involving treatment at around 290 °C for 6-12 min). There is a need to perform tests with a range of die channel lengths with small incremental increases (steps of < 5 mm) to further optimize quality within this optimal corner of the DoE space. This also suggests that it is necessary to carefully match the press channel length to the properties of the material to be pelletized.
- There may be a saddle point for the pelletization of material with a relatively high degree of torrefaction (>315 °C), at which durability increases and the production of fines decreases. If so, it would be possible to produce pellets of acceptable quality from material with a low initial moisture content.
- Higher moisture contents have strong adverse effects on the flow properties of torrefied materials during silo discharging and when conveying the material to the pellet mill.
- Die temperature control is an efficient way to overcome the discontinuous pellet production pattern that can arise, probably due to drying, when pelletizing straw and torrefied materials in a ring die that is continuously heated by friction as material is extruded through the press channels.
- Two innovative tools were developed for controlling and feed layer formation by indirect or direct cooling for pelletizing mills having stationary or rotating ring dies respectively.

5 Future research

5.1 Fixed die designs for effective test of torrefied materials

Bench studies based on press tools for production of single pellets do not fully simulate the full-scale pelletization process. An example is that the material is compressed against a blocking device on the bench whereas in a conventional pelletizing, small amounts of the feedstock material are added each time the roller passes over each press channel and the formed pellet inside the channel is pushed a bit further towards the outlet of the die. This is also evident by the pattern of material layers formed within the pellet, which is readily observed by breaking a pellet into two pieces by bending it. Single press tools produce layers that are oriented in a flat plane perpendicular to the pressing direction. Conversely, in conventional pellets of good quality, the plane of added layers are curved in towards the centre of the pellet, in the same direction as the pressing force - this curved plane indirectly shows that the friction between the particles and press channel wall in such cases is somewhat higher than that between particles in the centre of the pellets. It is therefore necessary to develop new research tools that enable experimental designs to be developed using small amounts of material but whose performance is more directly comparable to that of conventional industrial presses.

Future studies in this area will therefore focus on developing concepts for such tools, and particularly on exploring the potential of using fixed designs of experiments embedded in the design of the press channels of the die. In the Supplementary section to Paper IV, it was shown that each 1 mm increase in press channel length corresponded to an increase in bulk density of about 20 kg m^{-3}. It is thus possible that incorporating multiple different press channel lengths in a single die could reduce the time, cost, and amount of feedstock consumed during optimization experiments because it would be possible to perform experiments with multiple channel lengths without changing the die or

having start-up and close-down periods for every different press channel length to be tested.

Any such variation of individual press channel lengths will necessitate the development of devices for collecting, separating, and identifying the pellets produced through different channels. The idea is to use pellet mills having fixed dies and a rotating set of free rolling rollers. This opens up the possibility of collecting the pellets as they are produced and measuring pellet production through individual press channels. A prototype of this concept (shown in *Figure 15*) has already been tested successfully.

Figure 15. Prototype sampling device (8 × 3) for the SPC PP300 Compact Pelletizer (Photo: M Rudolfsson).

Another design variable relating to the press channel that could be optimized further is the inlet angle. The inlet angle increases the volume that must be compressed, and affects the amount of material that must be sheared into the channel. *Figure 16* shows a channel with an inlet angle of 45° relative to the channel's centre line, and the extra volume created by this angle relative to that for a theoretical press channel with an inlet angle of 0°. If this extra volume is fixed, the inlet angle can be adjusted to maintain a constant volume. This is indicated in *Figure 13A* by the tangent as a dashed curved line. By plugging channels, as shown in *Figure 16B*, it is possible to decrease the amount of material needed for experiments. Such plugging can be done in channel rows but then the rolls have to be narrowed down.

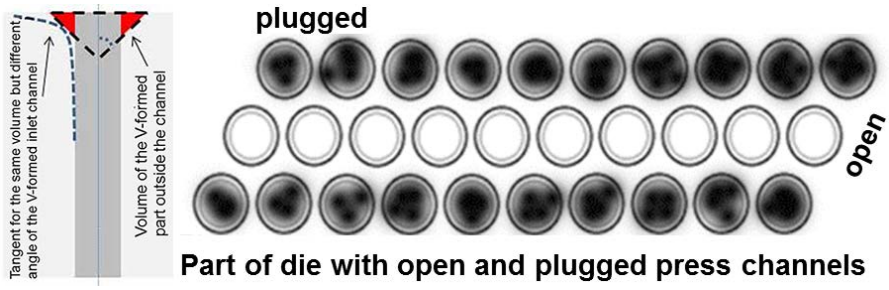

Figure 16. A: The dependence of the extra volume (red) on the inlet angle; B: a die design with three lines of press channels, of which only the centre line is used in initial studied to minimize the consumption of feedstock material.

Factors that can be varied in the design of individual press channels include the length, inlet angle and extra inlet volume.

Figure 17 shows a full factorial design featuring 30 channels having different inlet angles (e.g. 30, 45 and 60° opening angle), and press lengths (e.g. 28, 29, 30, 31 and 32 mm), with two levels of extra volume. The specified pressure lengths are centred around 30 mm on the basis of the results presented in Paper IV.

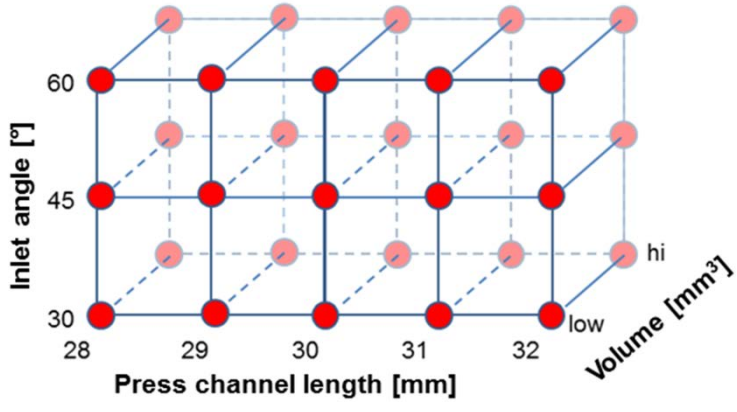

Figure 17. Full factorial design in which the press channels' lengths, inlet angles, and inlet volume are varied over five, three and two levels, respectively.

5.1.1 Variable roll friction

The free rollers that compress the material into a feed layer generate some friction that stresses the lateral adhesion of the compressed feed layer at the same time as it is sheared and pressed towards the press channel. It would be interesting to use separate motors for each roller and thereby control this friction. By adjusting the rollers' rotation to match their movement over the

feed layer, it may be possible to eliminate the influence of their friction. Such a device could also be used to increase the rollers' friction by setting the rotation speed lower than its natural rotation when in contact with a stable feed layer such that the rollers function as brakes; by gradually increasing the braking force applied in this way, it would be possible to evaluate the feed layer's lateral adhesion.

5.1.2 Nozzle injection

The results from Paper VI clearly show the extended abilities to widen the controls of the pelletization process by introducing innovative nozzle injections e.g. of water droplets direct into the press nip. This development may in its simple form revolutionize the controls of pellet mills having rotating dies and a fixed set of free rolling rollers.

These nozzles can be used to heat or cool the pelletizing process less than seconds before compression into a feed layer. Thus it may not be necessary to condition the material and a possible scenario is that nearly all variation of moisture content in the material is levelled out by compensatory injections of water. In an extreme case it may be possible to monitor mol of certain chemical structural groups e.g. O-H per kg dry mass (Kymäläinen *et al.*, 2015) and adjust moisture to optimal levels. Furthermore, it is also possible that there are new innovations to discover in the applications of using nozzles in pellet press mills having rotating dies (see *Figure 18*).

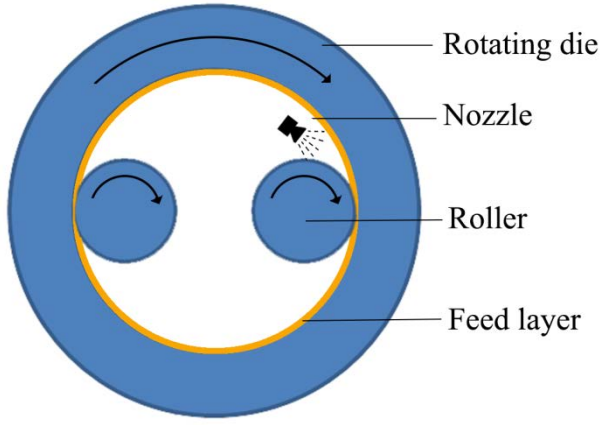

Figure 18. Example of placing nozzle for direct injections into the press nip.

Acknowledgements

Tack till min handledare Torbjörn Lestander för att du trodde på mig och plockade in mig som doktorand i dina projekt och för den hjälp och undervisning som jag fått under arbetets gång. Jag vill ge ett särskilt tack för det tålamod och den empati som du har visat mig under perioder då det inte gått så bra som det borde.

Tack till biträdande handledare Robert Samuelsson för att du tagit dig tid att läsa och kommentera och för att du hjälpt mig med en mängd statistiska funderingar. Särskilt uppskattar jag din saklighet som kan behövas.

Tack till biträdande handledare Linda Pommer för att som medförfattare hjälpt mig i skrivprocessen.

Tack till biträdande handledare Markus Broström för samarbeten som dock hamnat utanför avhandlingsarbetet med förhoppningar om framtida samarbeten. Låt oss pelletera!

Tack Sylvia Larsson för att du har varit mitt bollplank under doktorandarbetet och min vän före, under och efter doktorandarbetet.

Tack Mikael Thyrel för att du har gått före mig som doktorand och sopat banan. Du har varit till stor hjälp i mitt arbete men också hjälpt till att hålla humöret uppe med trevliga avbrott i arbetet.

Tack Eleonora Borén för dina heroiska insatser i den eviga kampen att submitta ”kombopeket”. Jag hoppas verkligen att det kommer några enklare papers framöver.

Tack Gunnar Kalén för all hjälp på BTC men också för att jag uppskattar att jobba tillsammans med dig.

Tack Markus Segerström för hjälp med analyser och provtagning på BTC.

Tack Håkan Örberg för din entusiasm och ditt engagemang!

Tack Ingemar Lindh, Martin Strandberg och Erik Sandström för torrefierat material, särskilt till Paper IV där er arbetsinsats var enorm för att få fram material.

Tack alla kollegor på institutionen för smått och stort!

Tack alla medförfattare; Eleonora Borén, Sylvia H. Larsson, Torbjörn A. Lestander, Ingemar Lindh (tidigare Olofsson), Anders Nordin, Linda Pommer, Robert Samuelsson, Wolfgang Stelte, Martin Strandberg (tidigare Nordwaeger), som alla hjälpt mig framåt i skrivprocessen.

Tack alla kompisar som gett mig ett liv utanför jobbet.

Tack till doktoranderna inom Bio4Energy.

Tack till finansiärerna som gjort detta doktorandprojekt möjligt: Energimyndigheten (projekt Future BioPellets 32747-1), EU FP7 (projekt SECTOR grant no. 282826), EU H2020−SPIRE−2014 (project Mobile and Flexible Industrial Processing of Biomass −MOBILE FLIP. Proposal number: 637020), FoU-rådet för SP Processum och Framtidens Bioraffinaderi, och den strategiska forskningsmiljön Bio4Energy utsedd av Sveriges regering.

Tack till Biofuel Technology Centre (BTC).

Tack till BioEndev för torrefierade material.

Tack till SP Energy Technology Center för material.

Tack Anders och Niklas för att ni inte har varit så intresserade av mitt jobb.

Tack mamma och pappa för er omtanke men kanske mest för att ni har låtit oss barn hålla på med allt möjligt hemma.

Slutligen vill jag tacka min familj: Stina, Greta, Kerstin och Erik för allt som ett jobb inte kan ge.

References

Alakangas, E. (2014). Deliverable No. D8.3 Graded thermally and densified biomass fuels, Development of the ISO 17225-8 standard. Production of Solid Sustainable Energy Carriers from Biomass by Means of Torrefaction. https://sector-project.eu/fileadmin/downloads/deliverables/SECTOR_Deliverable_8_3_VTT__Final-November2015.pdf 2014. (2016-03-03).

Allen, M.R., Frame, D.J., Huntingford, C., Jones, C.D., Lowe, J.A., Meinshausen, M. & Meinshausen, N. (2009). Warming caused by cumulative carbon emissions towards the trillionth tonne. *Nature,* 458(7242), pp. 1163-1166.

Axrup, L., Markides, K. & Nilsson, T. (2000). Using miniature diode array NIR spectrometers for analysing wood chips and bark samples in motion. *Journal of Chemometrics,* 14(5-6), pp. 561-572.

Beer, C., Reichstein, M., Tomelleri, E., Ciais, P., Jung, M., Carvalhais, N., Roedenbeck, C., Arain, M.A., Baldocchi, D., Bonan, G.B., Bondeau, A., Cescatti, A., Lasslop, G., Lindroth, A., Lomas, M., Luyssaert, S., Margolis, H., Oleson, K.W., Roupsard, O., Veenendaal, E., Viovy, N., Williams, C., Woodward, F.I. & Papale, D. (2010). Terrestrial Gross Carbon Dioxide Uptake: Global Distribution and Covariation with Climate. *Science,* 329(5993), pp. 834-838.

Bergman, P.C.A., Boersma, A.R., Zwart, R.W.R. & Kiel, J.H.A. (2005). Torrefaction for biomass co-firing in existing coal-fired power stations biocoal. *Report ECN-C-05-013, ECN, Petten, The Netherlands.*

Boerjan, W., Ralph, J. & Baucher, M. (2003). Lignin biosynthesis. *Annual Review of Plant Biology,* 54, pp. 519-546.

Bose, S.K., Francis, R.C., Govender, M., Bush, T. & Spark, A. (2009). Lignin content versus syringyl to guaiacyl ratio amongst poplars. *Bioresource Technology,* 100(4), pp. 1628-1633.

Boström, D., Skoglund, N., Grimm, A., Boman, C., Öhman, M., Broström, M. & Backman, R. (2012). Ash Transformation Chemistry during Combustion of Biomass. *Energy & Fuels,* 26(1), pp. 85-93.

Bourgois, J. & Guyonnet, R. (1988). Characterization and analysis of torrefied wood. *Wood Science and Technology,* 22(2), pp. 143-155.

Boutelje, J.B. (1966). On the anatomical structure, moisture content, density, shrinkage, and resin content of the wood in and around knots in Swedish pine (Pinus silvestris L.) and in Swedish spruce (Picea abies Karst.). *Svensk Papperstidning-Nordisk Cellulosa,* 69(1), pp. 1-&.

Chen, Y., Liu, B., Yang, H., Yang, Q. & Chen, H. (2014). Evolution of functional groups and pore structure during cotton and corn stalks torrefaction and its correlation with hydrophobicity. *Fuel,* 137, pp. 41-49.

Davies, T. (1998). The history of near infrared spectroscopic analysis: Past, present and future - "From sleeping technique to the morning star of spectroscopy". *Analusis,* 26(4), pp. M17-M19.

Di Blasi, C., Branca, C., Sarnataro, F.E. & Gallo, A. (2014). Thermal Runaway in the Pyrolysis of Some Lignocellulosic Biomasses. *Energy & Fuels,* 28(4), pp. 2684-2696.

Domalski, E.S. & Milne, T.A. (1987). Thermodynamic Data for Biomass Materials and Waste Components. The ASME Research Committee on Industrial and Municipal Wastes, New York: The American Society of Mechanical Engineers.

EN 14774-1:2009 Solid biofuels – Determination of moisture content – Oven dry method – Part 1: Total moisture – Reference method.

EN 14775:2009 Solid biofuels – Determination of ash content.

EN 14918:2009 Solid biofuels – Determination of calorific value.

EN 15103:2009 Solid biofuels - Determination of bulk density.

EN 15104:2011 Solid biofuels – Determination of total content of carbon, hydrogen and nitrogen – Instrumental methods.

EN 15148:2009 Solid biofuels – Determination of the content of volatile matter.

EN 15210-1:2009 Solid biofuels – Determination of mechanical durability of pellets and briquettes – Part 1: Pellets.

EN ISO 17225-1:2014 Solid biofuels -- Fuel specifications and classes -- Part 1: General requirements.

EPC (2015). ENplus Handbook, Part 1 – General Part. European Pellet Council (EPC). *European Biomass Association, Brussels, Belgium*.

Eriksson, L., Johansson, E., Kettaneh-Wold, N., Wikström, C. & Wold, S. (2008). *Design of Experiments: Principles and Applications*. Umeå, Sweden: Umetrics.

Ewanick, S.M., Thompson, W.J., Marquardt, B.J. & Bura, R. (2013). Real-time understanding of lignocellulosic bioethanol fermentation by Raman spectroscopy. *Biotechnology for Biofuels,* 6(1), pp. 1-8.

Faix, O., Fortmann, I., Bremer, J. & Meier, D. (1991). Thermal degradation products of wood. *European Journal of Wood and Wood Products,* 49(5), pp. 213-219.

Faix, O., Meier, D. & Fortmann, I. (1990). Thermal degradation products of wood. *European Journal of Wood and Wood Products,* 48(7), pp. 281-285.

Fink, H.P., Weigel, P., Purz, H.J. & Ganster, J. (2001). Structure formation of regenerated cellulose materials from NMMO-solutions. *Progress in Polymer Science*, 26(9), pp. 1473-1524.

Fisher, R.A. (1935). *The Design of Experiments*. 9th (1971). ed.

Friedlingstein, P., Andrew, R.M., Rogelj, J., Peters, G.P., Canadell, J.G., Knutti, R., Luderer, G., Raupach, M.R., Schaeffer, M., van Vuuren, D.P. & Le Quere, C. (2014). Persistent growth of CO2 emissions and implications for reaching climate targets. *Nature Geoscience*, 7(10), pp. 709-715.

Gaur, S. & Reed, T.B. (1995). *An Atlas of Thermal Data for Biomass and Other Fuels*: NREL/TB-433-7965, UC Category:1310, DE95009212, National Renewable Energy Laboratory, Golden, Colorado, USA.

Gerber, L., Eliasson, M., Trygg, J., Moritz, T. & Sundberg, B. (2012). Multivariate curve resolution provides a high-throughput data processing pipeline for pyrolysis-gas chromatography/mass spectrometry. *Journal of Analytical and Applied Pyrolysis*, 95, pp. 95-100.

Gibson, L.J. (2012). The hierarchical structure and mechanics of plant materials. *Journal of the Royal Society Interface*, 9(76), pp. 2749-2766.

Golub, G.H. & Reinsch, C. (1970). Singular value decomposition and least squares solutions *Numerische Mathematik*, 14(5), pp. 403-&.

Grigiante, M. & Antolini, D. (2015). Mass yield as guide parameter of the torrefaction process. An experimental study of the solid fuel properties referred to two types of biomass. *Fuel*, 153, pp. 499-509.

Hatfield, R.D. (1993). *Cell-wall polysaccharide interactions and degradability*. (Forage Cell Wall Structure and Digestibility. Madison: Amer Soc Agronomy. Available from: <Go to ISI>://WOS:A1993BY63Z00012.

Holm, J.K., Henriksen, U.B., Wand, K., Hustad, J.E. & Posselt, D. (2007). Experimental verification of novel pellet model using a single pelleter unit. *Energy & Fuels*, 21(4), pp. 2446-2449.

IPCC (2013). Summary for Policymakers. In: Climate Change 2013: The Physical Science Basis. Contribution of Working Group I to the Fifth Assessment Report of the Intergovernmental Panel on Climate Change.(Stocker, T.F., D. Qin, G.-K. Plattner, M. Tignor, S.K. Allen, J. Boschung, A. Nauels, Y. Xia, V. Bex and P.M. Midgley (eds.).), pp. Cambridge University Press, Cambridge, United Kingdom and New York, NY, USA.

Jarvinen, T. & Agar, D. (2014). Experimentally determined storage and handling properties of fuel pellets made from torrefied whole-tree pine chips, logging residues and beech stem wood. *Fuel*, 129, pp. 330-339.

Jirjis, R. (1995). Storage and drying of wood fuel. *Biomass & Bioenergy*, 9(1-5), pp. 181-190.

Johnson, E. (2009). Goodbye to carbon neutral: Getting biomass footprints right. *Environmental Impact Assessment Review*, 29(3), pp. 165-168.

Jung, M., Reichstein, M., Margolis, H.A., Cescatti, A., Richardson, A.D., Arain, M.A., Arneth, A., Bernhofer, C., Bonal, D., Chen, J.Q., Gianelle, D., Gobron, N., Kiely, G., Kutsch, W., Lasslop, G., Law, B.E., Lindroth, A., Merbold, L., Montagnani, L., Moors, E.J., Papale, D., Sottocornola, M.,

Vaccari, F. & Williams, C. (2011). Global patterns of land-atmosphere fluxes of carbon dioxide, latent heat, and sensible heat derived from eddy covariance, satellite, and meteorological observations. *Journal of Geophysical Research-Biogeosciences*, 116.

Kaliyan, N. & Morey, R.V. (2009). Factors affecting strength and durability of densified biomass products. *Biomass & Bioenergy*, 33(3), pp. 337-359.

Kenney, K.L., Smith, W.A., Gresham, G.L. & Westover, T.L. (2013). Understanding biomass feedstock variability. *Biofuels*, 4(1), pp. 111-127.

Kim, J.Y., Hwang, H., Park, J., Oh, S. & Choi, J.W. (2014). Predicting structural change of lignin macromolecules before and after heat treatment using the pyrolysis-GC/MS technique. *Journal of Analytical and Applied Pyrolysis*, 110, pp. 305-312.

Klemm, D., Heublein, B., Fink, H.P. & Bohn, A. (2005). Cellulose: Fascinating biopolymer and sustainable raw material. *Angewandte Chemie-International Edition*, 44(22), pp. 3358-3393.

Koppejan, J., Sokhansanj, S., Melin, S. & Madrali, S. (2012). Status overview of torrefaction technologies. International Energy Agency, IEA Bioenergy Task 32 report. *IEA Bioenergy Task 32 report*.

Kummamuru, B.V. (2015). WBA Global Bioenergy Statistics 2015. *World Bioenergy Association 2015*.

Kymäläinen, M., Rautkari, L. & Hill, C.A.S. (2015). Sorption behaviour of torrefied wood and charcoal determined by dynamic vapour sorption. *Journal of Materials Science*, 50(23), pp. 7673-7680.

Larsson, S.H., Rudolfsson, M., Nordwaeger, M., Olofsson, I. & Samuelsson, R. (2013). Effects of moisture content, torrefaction temperature, and die temperature in pilot scale pelletizing of torrefied Norway spruce. *Applied Energy*, 102, pp. 827-832.

Larsson, S.H., Rudolfsson, M., Thyrel, M., Orberg, H., Kalen, G., Wallin, M. & Lestander, T.A. (2012). Temperature controlled feed layer formation in biofuel pellet production. *Fuel*, 94(1), pp. 81-85.

Larsson, S.H., Thyrel, M., Geladi, P. & Lestander, T.A. (2008). High quality biofuel pellet production from pre-compacted low density raw materials. *Bioresource Technology*, 99(15), pp. 7176-7182.

Lestander, T.A. (2013). Pellet and briquette production. In: Dahlquist, E. (ed. *Technologies for Converting Biomass to Useful Energy: Combustion, gasification, pyrolysis, torrefaction and fermentation*. Leiden, The Netherlands: CRC Press/Balkema, pp. 345-355.

Lestander, T.A., Geladi, P., Larsson, S.H. & Thyrel, M. (2012a). Near infrared image analysis for online identification and separation of wood chips with elevated levels of extractives. *Journal of near Infrared Spectroscopy*, 20(5), pp. 591-599.

Lestander, T.A., Johnsson, B. & Grothage, M. (2009). NIR techniques create added values for the pellet and biofuel industry. *Bioresource Technology*, 100(4), pp. 1589-1594.

Lestander, T.A., Lundstrom, A. & Finell, M. (2012b). Assessment of biomass functions for calculating bark proportions and ash contents of refined biomass fuels derived from major boreal tree species. *Canadian Journal of Forest Research-Revue Canadienne De Recherche Forestiere,* 42(1), pp. 59-66.

Lestander, T.A. & Rhen, C. (2005). Multivariate NIR spectroscopy models for moisture, ash and calorific content in biofuels using bi-orthogonal partial least squares regression. *Analyst,* 130(8), pp. 1182-1189.

Li, H., Liu, X.H., Legros, R., Bi, X.T.T., Lim, C.J. & Sokhansanj, S. (2012). Pelletization of torrefied sawdust and properties of torrefied pellets. *Applied Energy,* 93, pp. 680-685.

Li, X.L., Sun, C.J., Zhou, B.X. & He, Y. (2015). Determination of Hemicellulose, Cellulose and Lignin in Moso Bamboo by Near Infrared Spectroscopy. *Scientific Reports,* 5.

Lindh, I., Strandberg, M., Burman, J., Pommer, L., Sjöström, M., Sandström, E. & Nordin, A. (2016). Design and implementation of a continuous flow reactor for low temperature thermal conversion of biomass. . *In print.*

Mante, O.D., Amidon, T.E., Stipanovic, A. & Babu, S.P. (2014). Integration of biomass pretreatment with fast pyrolysis: An evaluation of electron beam (EB) irradiation and hot-water extraction (HWE). *Journal of Analytical and Applied Pyrolysis,* 110, pp. 44-54.

McGlade, C. & Ekins, P. (2014). Un-burnable oil: An examination of oil resource utilisation in a decarbonised energy system. *Energy Policy,* 64, pp. 102-112.

Meinshausen, M., Meinshausen, N., Hare, W., Raper, S.C.B., Frieler, K., Knutti, R., Frame, D.J. & Allen, M.R. (2009). Greenhouse-gas emission targets for limiting global warming to 2 degrees C. *Nature,* 458(7242), pp. 1158-U96.

Melkior, T., Jacob, S., Gerbaud, G., Hediger, S., Le Pape, L., Bonnefois, L. & Bardet, M. (2012). NMR analysis of the transformation of wood constituents by torrefaction. *Fuel,* 92(1), pp. 271-280.

Meng, J., Park, J., Tilotta, D. & Park, S. (2012). The effect of torrefaction on the chemistry of fast-pyrolysis bio-oil. *Bioresource Technology,* 111, pp. 439-446.

Miles, T.R., Baxter, L.L., Bryers, R.W., Jenkins, B.M. & Oden, L.L. (1996). Boiler deposits from firing biomass fuels. *Biomass & Bioenergy,* 10(2-3), pp. 125-138.

Mosier, N., Wyman, C., Dale, B., Elander, R., Lee, Y.Y., Holtzapple, M. & Ladisch, M. (2005). Features of promising technologies for pretreatment of lignocellulosic biomass. *Bioresource Technology,* 96(6), pp. 673-686.

Murphey, W.K. & Masters, K.R. (1978). Gross heat of combustion of northern red oak (Quercus rubra L.) chemical components. *Wood Science,* 10(3), pp. 139-141.

NOAA (2015). National Centers for Environmental Information, State of the Climate: Global Analysis for Annual 2014. http://www.ncdc.noaa.gov/sotc/global/201413.

Nordin, A., Pommer, L., Nordwaeger, M. & Olofsson, I. (2013). Biomass conversion through torrefaction. In: Dahlquist, E. (ed. *Technologies for Converting Biomass to Useful Energy: Combustion, Gasification, Pyrolysis, Torrefaction and Fermentation*. (Sustainable Energy Developments, 4), pp. 217-244. Available from: <Go to ISI>://WOS:000351079400009.

Normark, M., Winestrand, S., Lestander, T.A. & Jonsson, L.J. (2014). Analysis, pretreatment and enzymatic saccharification of different fractions of Scots pine. *Bmc Biotechnology*, 14.

Obernberger, I., Brunner, T. & Barnthaler, G. (2006). Chemical properties of solid biofuels - significance and impact. *Biomass & Bioenergy*, 30(11), pp. 973-982.

Obernberger, I. & Thek, G. (2010). *The Pellet Handbook.* London: Earthscan Ltd.

Offrion, V.F.O. (1900). Improvments in the process of and apparatus for rationally and continuously treating or torrefying coffee. Patent GB 190001714.

Osborne (1993). *Practical NIR spectroscopy with applications in food and beverage analysis.* 2nd. ed. Harlow, Essex, England: Longman Scientific & Technical.

Park, J., Meng, J.J., Lim, K.H., Rojas, O.J. & Park, S. (2013). Transformation of lignocellulosic biomass during torrefaction. *Journal of Analytical and Applied Pyrolysis*, 100, pp. 199-206.

Pearson, K. (1901). On lines and planes of closest fit to systems of points in space. *Philos. Mag.*, Series 6, vol. 2, pp. 559-572.

Peng, J.H., Bi, H.T., Lim, C.J. & Sokhansanj, S. (2013). Study on Density, Hardness, and Moisture Uptake of Torrefied Wood Pellets. *Energy & Fuels*, 27(2), pp. 967-974.

Peng, J.H., Wang, J.S., Bi, X.T., Lim, C.J., Sokhansanj, S., Peng, H.C. & Jia, D.N. (2015). Effects of thermal treatment on energy density and hardness of torrefied wood pellets. *Fuel Processing Technology*, 129, pp. 168-173.

Phanphanich, M. & Mani, S. (2011). Impact of torrefaction on the grindability and fuel characteristics of forest biomass. *Bioresource Technology*, 102(2), pp. 1246-1253.

Pietsch, W. (ed.) (2002). *Agglomeration processes - phenomena, technologies, equipment*. Weinheim: Wiley-VCH.

prEN ISO 17225-8 Solid biofuels - Fuel specifications and classes - Part 8: Graded thermally treated and densified biomass fuels (ISO/DIS 17225-8:2016).

Prins, M.J., Ptasinski, K.J. & Janssen, F. (2006). Torrefaction of wood - Part 2. Analysis of products. *Journal of Analytical and Applied Pyrolysis*, 77(1), pp. 35-40.

Ragauskas, A.J., Williams, C.K., Davison, B.H., Britovsek, G., Cairney, J., Eckert, C.A., Frederick, W.J., Hallett, J.P., Leak, D.J., Liotta, C.L., Mielenz, J.R.,

Murphy, R., Templer, R. & Tschaplinski, T. (2006). The path forward for biofuels and biomaterials. *Science*, 311(5760), pp. 484-489.

REN21 (2015). *Renewables 2015 Global Status Report*. Paris: REN21 Secretariat.

Repellin, V., Govin, A., Rolland, M. & Guyonnet, R. (2010). Energy requirement for fine grinding of torrefied wood. *Biomass & Bioenergy*, 34(7), pp. 923-930.

Ruddiman, W.F., Ellis, E.C., Kaplan, J.O. & Fuller, D.Q. (2015). Defining the epoch we live in. *Science*, 348(6230), pp. 38-39.

Rumpf, H. (1962). The Strength of Granules and Agglomerates. In: Knepper, W.A. (ed. *Agglomeration* Interscience, New York.

Ryu, Y., Baldocchi, D.D., Kobayashi, H., van Ingen, C., Li, J., Black, T.A., Beringer, J., van Gorsel, E., Knohl, A., Law, B.E. & Roupsard, O. (2011). Integration of MODIS land and atmosphere products with a coupled-process model to estimate gross primary productivity and evapotranspiration from 1 km to global scales. *Global Biogeochemical Cycles*, 25.

Samuelsson, R., Larsson, S.H., Thyrel, M. & Lestander, T.A. (2012). Moisture content and storage time influence the binding mechanisms in biofuel wood pellets. *Applied Energy*, 99, pp. 109-115.

Sasai, T., Okamoto, K., Hiyama, T. & Yamaguchi, Y. (2007). Comparing terrestrial carbon fluxes from the scale of a flux tower to the global scale. *Ecological Modelling*, 208(2-4), pp. 135-144.

Schneider, S.H. (2004). Abrupt non-linear climate change, irreversibility and surprise. *Global Environmental Change-Human and Policy Dimensions*, 14(3), pp. 245-258.

Shang, L., Nielsen, N.P.K., Dahl, J., Stelte, W., Ahrenfeldt, J., Holm, J.K., Thomsen, T. & Henriksen, U.B. (2012). Quality effects caused by torrefaction of pellets made from Scots pine. *Fuel Processing Technology*, 101, pp. 23-28.

Shang, L., Nielsen, N.P.K., Stelte, W., Dahl, J., Ahrenfeldt, J., Holm, J.K., Arnavat, M.P., Bach, L.S. & Henriksen, U.B. (2014). Lab and Bench-Scale Pelletization of Torrefied Wood Chips-Process Optimization and Pellet Quality. *Bioenergy Research*, 7(1), pp. 87-94.

Sharma, R.K., Wooten, J.B., Baliga, V.L., Lin, X., Geoffrey Chan, W. & Hajaligol, M.R. (2004). Characterization of chars from pyrolysis of lignin. *Fuel*, 83(11–12), pp. 1469-1482.

Sheikh, M.M.I., Kim, C.-H., Park, H.-J., Kim, S.-H., Kim, G.-C., Lee, J.-Y., Sim, S.-W. & Kim, J.W. (2013). Effect of torrefaction for the pretreatment of rice straw for ethanol production. *Journal of the Science of Food and Agriculture*, 93(13), pp. 3198-3204.

Shen, D.K., Gu, S. & Bridgwater, A.V. (2010). The thermal performance of the polysaccharides extracted from hardwood: Cellulose and hemicellulose. *Carbohydrate Polymers*, 82(1), pp. 39-45.

Sheppard, N., Willis, H.A. & Rigg, J.C. (1985). Names, symbols, definitions and units of quantities in optical spectroscopy. *Pure and Applied Chemistry*, 57(1), pp. 105-120.

Shoulaifar, T.K., DeMartini, N., Ivaska, A., Fardim, P. & Hupa, M. (2012). Measuring the concentration of carboxylic acid groups in torrefied spruce wood. *Bioresource Technology*, 123, pp. 338-343.

Sikkema, R., Steiner, M., Junginger, M., Hiegl, W., Hansen, M.T. & Faaij, A. (2011). The European wood pellet markets: current status and prospects for 2020. *Biofuels Bioproducts & Biorefining-Biofpr*, 5(3), pp. 250-278.

Skoog, D.A. (1985). *Principles of Instrumental Analysis*. Third ed: Saunders Coll. Publ.

Solomon, S., Plattner, G.K., Knutti, R. & Friedlingstein, P. (2009). Irreversible climate change due to carbon dioxide emissions. *Proceedings of the National Academy of Sciences of the United States of America*, 106(6), pp. 1704-1709.

Steffen, W., Richardson, K., Rockstrom, J., Cornell, S.E., Fetzer, I., Bennett, E.M., Biggs, R., Carpenter, S.R., de Vries, W., de Wit, C.A., Folke, C., Gerten, D., Heinke, J., Mace, G.M., Persson, L.M., Ramanathan, V., Reyers, B. & Sorlin, S. (2015). Planetary boundaries: Guiding human development on a changing planet. *Science*, 347(6223), pp. 736-+.

Stelte, W., Clemons, C., Holm, J.K., Ahrenfeldt, J., Henriksen, U.B. & Sanadi, A.R. (2012). Fuel Pellets from Wheat Straw: The Effect of Lignin Glass Transition and Surface Waxes on Pelletizing Properties. *Bioenergy Research*, 5(2), pp. 450-458.

Stelte, W., Holm, J.K., Sanadi, A.R., Barsberg, S., Ahrenfeldt, J. & Henriksen, U.B. (2011). A study of bonding and failure mechanisms in fuel pellets from different biomass resources. *Biomass & Bioenergy*, 35(2), pp. 910-918.

Stelte, W., Nielsen, N.P.K., Hansen, H.O., Dahl, J., Shang, L. & Sanadi, A.R. (2013). Pelletizing properties of torrefied wheat straw (Reprinted from BIOMASS & BIOENERGY, vol 49, pg 214, 2013). *Biomass & Bioenergy*, 53, pp. 105-112.

Stephen, J.D., Mabee, W.E. & Saddler, J.N. (2010). Biomass logistics as a determinant of second-generation biofuel facility scale, location and technology selection. *Biofuels Bioproducts & Biorefining-Biofpr*, 4(5), pp. 503-518.

Still, C.J., Berry, J.A., Collatz, G.J. & DeFries, R.S. (2003). Global distribution of C-3 and C-4 vegetation: Carbon cycle implications. *Global Biogeochemical Cycles*, 17(1).

Strandberg, M., Olofsson, I., Pommer, L., Wiklund-Lindstrom, S., Aberg, K. & Nordin, A. (2015). Effects of temperature and residence time on continuous torrefaction of spruce wood. *Fuel Processing Technology*, 134, pp. 387-398.

Strömberg, B. & Herstad Svärd, S. (2012). *Bränslehandboken*. Stockholm: Värmeforsk serviceaktiebolag.

Sugiyama, J., Harada, H., Fujiyoshi, Y. & Uyeda, N. (1985). Lattice images from ultrathin sections of cellulose microfibrils in the cell-wall of Valonia macrophysa Kütz. *Planta*, 166(2), pp. 161-168.

Svebio (2016). Bioenergy data. *https://www.svebio.se/english/bioenergy-data*.

Tao, G., Geladi, P., Lestander, T.A. & Xiong, S. (2012a). Biomass properties in association with plant species and assortments. II: A synthesis based on literature data for ash elements. *Renewable & Sustainable Energy Reviews*, 16(5), pp. 3507-3522.

Tao, G., Lestander, T.A., Geladi, P. & Xiong, S. (2012b). Biomass properties in association with plant species and assortments I: A synthesis based on literature data of energy properties. *Renewable & Sustainable Energy Reviews*, 16(5), pp. 3481-3506.

Thiel, F.C. (1897). New or improved roaster or torrefier for coffee and other vegetable substances. Patent GB 18971065.

Thyrel, M. (2014). *Spectroscopic characterization of lignocellulosic biomass.* Diss. Umeå: Sveriges lantbruksuniversitet.

Thyrel, M., Samuelsson, R., Finell, M. & Lestander, T.A. (2013). Critical ash elements in biorefinery feedstock determined by X-ray spectroscopy. *Applied Energy*, 102, pp. 1288-1294.

Tumuluru, J.S., Wright, C.T., Hess, J.R. & Kenney, K.L. (2011). A review of biomass densification systems to develop uniform feedstock commodities for bioenergy application. *Biofuels Bioproducts & Biorefining-Biofpr*, 5(6), pp. 683-707.

UN (2013). Department of Economic and Social Affairs, Population Division. *World Population Prospects: The 2012 Revision, Highlights and Advance Tables*, Working Paper No. ESA/P/WP.228.

UNFCCC (2015). Adoption of the Paris Agreement. United Nations Framework Convention on Climate Change. *FCCC/CP/2015/L.9/Rev.1, pp:1-32.*

Walker, J. (2006). *Primary wood processing – principles and practice.* . 2nd. ed. Dordrecht, The Nederlands.: Springer.

Wang, G.L., Silva, R.B., Azevedo, J.L.T., Martins-Dias, S. & Costa, M. (2014). Evaluation of the combustion behaviour and ash characteristics of biomass waste derived fuels, pine and coal in a drop tube furnace. *Fuel*, 117, pp. 809-824.

Vassilev, S.V., Baxter, D., Andersen, L.K. & Vassileva, C.G. (2010). An overview of the chemical composition of biomass. *Fuel*, 89(5), pp. 913-933.

Vassilev, S.V., Baxter, D., Andersen, L.K., Vassileva, C.G. & Morgan, T.J. (2012). An overview of the organic and inorganic phase composition of biomass. *Fuel*, 94(1), pp. 1-33.

Weiss, N.D., Farmer, J.D. & Schell, D.J. (2010). Impact of corn stover composition on hemicellulose conversion during dilute acid pretreatment and enzymatic cellulose digestibility of the pretreated solids. *Bioresource Technology*, 101(2), pp. 674-678.

Wen, J.L., Sun, S.L., Yuan, T.Q., Xu, F. & Sun, R.C. (2014). Understanding the chemical and structural transformations of lignin macromolecule during torrefaction. *Applied Energy*, 121, pp. 1-9.

Werner, K., Pommer, L. & Brostrom, M. (2014). Thermal decomposition of hemicelluloses. *Journal of Analytical and Applied Pyrolysis*, 110, pp. 130-137.

Westover, T.L. (2013). *Analysis of ash composition using laser-induced breakdown spectroscopy (LIBS)*. Idaho Falls, Idaho: Idaho National Laboratory, Biofuels and Renewable Energy Technologies Division.

Witt, J., Schaubach, K., Ristola, M., Bellmann, V. & Thrän, D. (2015). Deliverable No. D1.3 Final report based on Conference Proceedings of Final Project Conference. Production of Solid Sustainable Energy Carriers from Biomass by Means of Torrefaction. https://sector-project.eu/fileadmin/downloads/deliverables/FINAL_SECTOR_D1.3_and_Annex.pdf 2015. (2016-03-03).

Wold, H. (1966). Nonlinear estimation by iterative least squares procedures. In: David, F.N. (ed. *Research Papers in Statistics. Festschrift for J. Neyman* Wiley, New York, pp. 411-444.

Wold, H. (1975). Path modelswith latent variables: the NIPALS approach. In: Quantitative Sociology. *Academic Press, New York, USA. p 305-357*.

Yan, H., Wang, S.-q., Billesbach, D., Oechel, W., Bohrer, G., Meyers, T., Martin, T.A., Matamala, R., Phillips, R.P., Rahman, F., Yu, Q. & Shugart, H.H. (2015). Improved global simulations of gross primary product based on a new definition of water stress factor and a separate treatment of C3 and C4 plants. *Ecological Modelling*, 297, pp. 42-59.

Yuan, W., Liu, S., Yu, G., Bonnefond, J.-M., Chen, J., Davis, K., Desai, A.R., Goldstein, A.H., Gianelle, D., Rossi, F., Suyker, A.E. & Verma, S.B. (2010). Global estimates of evapotranspiration and gross primary production based on MODIS and global meteorology data. *Remote Sensing of Environment*, 114(7), pp. 1416-1431.

Yvan, S. (1985). Process for converting ligneous matter of vegetable origin by torrefaction, and product obtained thereby. *United States Patent No. 4,553,978*.

Zevenhoven-Onderwater, M., Blomquist, J.P., Skrifvars, B.J., Backman, R. & Hupa, M. (2000). The prediction of behaviour of ashes from five different solid fuels in fluidised bed combustion. *Fuel*, 79(11), pp. 1353-1361.

Zhao, M.S., Heinsch, F.A., Nemani, R.R. & Running, S.W. (2005). Improvements of the MODIS terrestrial gross and net primary production global data set. *Remote Sensing of Environment*, 95(2), pp. 164-176.

Zheng, A., Zhao, Z., Chang, S., Huang, Z., Zhao, K., Wei, G., He, F. & Li, H. (2015). Comparison of the effect of wet and dry torrefaction on chemical structure and pyrolysis behavior of corncobs. *Bioresource Technology*, 176, pp. 15-22.